

Engineering of Therapeutic Proteins: Applications to Cancer and Fribrodysplasia
Ossificans Progressiva

A Senior Honors Thesis

Presented in Partial Fulfillment of the Requirements for graduation
with research distinction in Biochemistry in the undergraduate colleges
of The Ohio State University

By

Cynthia Renee Campbell

The Ohio State University
May 2016

Committee:

Dr. Thomas J. Magliery, Advisor

Dr. Noel M. Paul

Dr. Gregory Booton

Copyright

Cynthia Renee Campbell

2016

Abstract

The Notch signaling pathway has been implicated in many diseases due to deregulation in its role in many cellular processes. One major area of concern is its hand in cell proliferation of tumors in cancerous tissues. The extracellular Delta-like Ligand 1 (DLL1) that binds to Notch receptors has become a focus in recent studies in mice models by the Dikov Laboratory and their results suggest that a soluble cluster of a multivalent DLL1 may have therapeutic usage to suppress tumor growth. However, these DLL1 clusters are heterogeneous collages that are not suitable for in vivo testing or therapeutic drug creation. As a result, the Magliery Laboratory is expressing a variety of homogeneous DLL proteins. Through optimizing different expression, purification, and refolding techniques, numerous refolded DLL1 proteins have already been synthesized. These include a long ligand with three Epidermal Growth Factor (EGF) domains, a shortened ligand two EGF repeated domains, ligands with and without the N-terminal MNLL domain, and ligands with and without a C-terminal cysteine for PEGylation. A polyvalent structure of DLL1 ideally would have the potential to prevent tumor proliferation and cause apoptosis in cancerous tissues. Currently, we are optimizing the crosslinking of these fragments with PEG based linkers to make homogeneous, polyvalent constructs. Also, in vitro binding studies of these various proteins to the Notch receptor are underway in order to confirm the importance of each domain from our findings in the in vivo assays by the Dikov Laboratory.

Fibrodysplasia Ossificans Progressiva (FOP) is a progressive heterotopic endochondral ossification (HEO) that results in bone formation in atypical extra-skeletal

locations. A non-lethal heterozygous mutation in the activin receptor IA/activin-like kinase-2 (AVCR1/ALK2) was identified as a potential therapeutic target as this mutation exists in all cases of FOP. This complex is affiliated with bone morphogenetic protein (BMP) signaling receptor complexes, which is known to play a major role in bone and cartilage formation among other functions. Since the over-activity of the BMP signaling pathway is attributed as the cause to this disease, a possible inhibitor for excessive bone growth is a protein called Noggin, which binds and sequesters BMPs. Also a region of CV-2 called VWC has been found to bind to a different site on BMPs and sequester BMPs. In order to execute a number of different binding studies, optimizing the expression and purification of AVCR, BMP2, BMP4, Noggin, and VWC has been the initial goals of the Magliery Lab.

Dedicated to Darby High and Tori Fantozzi. Don't stop, don't give up.

Acknowledgments

Dr. Thomas J. Magliery – Principal Investigator/Advisor – Ohio State University
Departments of Chemistry and Biochemistry

Dr. Noel M. Paul – Oral Exam Committee – Ohio State University Department of
Chemistry and Biochemistry

Dr. Gregory Booton – Oral Exam Committee – Ohio State University Department of
Molecular Genetics

Dr. Nicholas W. Callahan – Postdoctoral Associate

Dr. Brandon Sullivan – Postdoctoral Associate

Nicholas Emerson Long – OSBP Graduate Student

Sidharth Mohan – Graduate Student

Kimberly Stephany – Research Assistant

All the members of Magliery Lab for their advice, guidance, and lively community.

Funding

Undergraduate Research Scholarship through the Arts and Sciences College

Undergraduate Education Summer Research Fellowships

Drug Discovery Initiative (DDI)

Vita

2012 Hudson High School, Hudson, Ohio
2015-2016 Undergraduate Researcher, Department of
Chemistry and Biochemistry, The Ohio
State University

Fields of Study

Major Field: Biochemistry
Minor Field: Forensic Science
Area of Distinction: Biochemistry

Table of Contents

Abstract	2
Dedication	3
Acknowledgements	4
Vita	5
Chapter 1: Introduction	8
1.1 Contributions and Protein Engineering Goals	8
1.2 Notch Project Background	9
1.3 FOP Background	13
1.4 Approaches	17
1.4.1 Specific to Notch Project.....	17
1.4.2 Specific to FOP Project	18
Chapter 2: Materials and Methods	19
2.1 Cloning	19
2.1.1 General Polymerase Chain Reactions (PCR) Procedure	19
2.1.2 General Ligation Reaction Procedure	19
2.1.3 Cloning MBP and PelB-MBP Notch Constructs	20
2.1.4 Cloning MNNL Notch Constructs	22
2.1.5 Cloning FOP Related Constructs	24
2.2 Expression, Lysing, Purification	26
2.2.1 Expression and Lysing General Protocol	26
2.2.2 Notch Protein Expression and Purification Protocol	27
2.2.3 FOP Related Protein Expression between Cell Lines	30
2.2.4 FOP Related Protein Expression among Variants	31
2.3 Conjugation	32
2.3.1 Cloning	32
2.4 Analysis.....	33
2.4.1 Western Blot Protocol	19
2.4.2 Matrix-Assisted Laser Desorption/Ionization Mass Spectrometry	19
Chapter 3: Results and Discussion	35
3.1 Notch Project	35
3.1.1 Variants (PelB)-His-TEV-DSL-EGF1-EGF2-(EGF3).....	35
3.1.2 Variants (PelB)-MBP-His-TEV-DSL-EGF1-EGF2-(EGF3)	41
3.1.3 Variants His-TEV-MNNL-DSL-EGF1-EGF2-EGF3	46
3.1.4 Conjugation of Notch C-terminal Cysteine Constructs	48
3.2 FOP Project	50
3.2.1 Cloning and Expression Experiments of FOP Related Constructs	50
3.2.2 PelB-His-tagged vs His-tagged vs Untagged	51
Conclusion and Future Directions	55
References	56

Tables

Table 1 MBP PCR templates and primers	20
Table 2 PelB-MBP PCR templates and primers	22
Table 3 MNNL PCR templates and primers	23
Table 4 DLL1 construct variants	28
Table 5 FOP related proteins and variants	30

Figures

Figure 1 DLL1 expression in human and mice in normal and tumor tissues	10
Figure 2 Notch signaling pathway	11
Figure 3 Askeletal bone growth typical in FOP	13
Figure 4 General function of FOP proteins	15
Figure 5 pHLIC-MBP Notch plasmid map	21
Figure 6 pHLIC Notch plasmid map	21
Figure 7 pHLIC MNNL Notch plasmid map	23
Figure 8 pHLIC-PELB FOP plasmid map	25
Figure 9 Testing PelB leader sequence addition	36
Figure 10 Western blot of PelB gel	37
Figure 11 Re-folding murine constructs	38
Figure 12 TEV-cleaved murine samples	39
Figure 13 Collaboration with Dikov lab	40
Figure 14 Origami cells	41
Figure 15 MBP variants on 1 st nickel column	42
Figure 16 MBP variants on 2 nd nickel column	43
Figure 17 MBP vs PelB-MBP purification	44
Figure 18 MALDI-TOF MS of MBP vs PelB-MBP variants	45
Figure 19 MNNL expression	47
Figure 20 Purification of MNNL via Tev-cleavage attempt	47
Figure 21 Over-PEGylation of Human 123	49
Figure 22 PEG molecules used for future crosslinking	49
Figure 23 FOP related protein His6 only constructs	50
Figure 24 Expression of FOP related constructs in BL21 (DE3) cells	51
Figure 25 BMP2 expression in BL21 (DE3) cells	52
Figure 26 BMP4 expression in BL21 (DE3) cells	52
Figure 27 NOGGIN expression in BL21 (DE3) cells	53
Figure 28 VWC expression in C41 (DE3) cells	53
Figure 29 ACVR expressed in C41 (DE3) cells	54

Chapter 1: Introduction

1.1 Contributions and Protein Engineering Goals

From cloning to expression, I have worked on the initial basic work on both the Notch project with Nicholas Emerson Long started by Dr. Brandon Sullivan and the FOP project with Dr. Nicholas W. Callahan. In the study of two debilitating diseases, cancer and fibrodysplasia ossificans progressiva (FOP), the possibility of further examining these diseases through protein engineering is the perspective the Magliery lab has decided to take up as possible solutions to these diseases. The Notch signaling pathway has been implicated in many diseases due to deregulation in its role in many cellular processes. One major area of concern is its hand in cell proliferation of tumors in cancerous tissues. The Notch signaling pathway contains a transmembrane receptor that requires extracellular substrate binding in order to induce the cascading effect inside the cell. Likewise, the same fundamental idea of what causes the crippling FOP disease where bone tissue grows and accumulates in askeletal regions. The atypical bone growth from FOP is triggered by a protein coded from a mutated ACVR1 gene. This mutation leads to the surplus release of internal signaling to stimulate the bone morphogenetic signaling pathway for every external binding on the ACVR1 transmembrane protein. Since cancer is an increasingly growing phenomenon that amasses much attention from the scientific community, rarer diseases such as FOP that share similar fundamental triggers that create these health problems can use similar methods of solving the symptomatic onsets. Because past research on both of these topics have led to the interest in the characteristics

of these proteins that cause these diseases, protein engineering and characterization have been main foci in the Magliery lab.

1.2 Notch Project Background

Extensive examinations of the Notch signaling pathway have been performed due to its vast implications in multiple diseases. The Notch signaling pathway, known to control cell-fate specification events and implicated in numerous fundamental regulatory processes, is attributed to many developmental defects that lead to a range of known diseases (Fortini 2009). The discovery of the Notch signaling pathway in 1916 was first observed in X-linked, dominant allele found on the chromosomes of *Drosophila* genetic mutants, which exhibited missing tissue in irregular notches on the tips of their wing blades (Mohr, 1919; Morgan and Bridges, 1916). Then in 1940, Poulson found that a complete loss in Notch gene activity caused fatal hyperplasia from cell proliferation of the embryonic nervous system. As more research was done on the role of Notch, cell proliferation, apoptosis, and the epithelial-mesenchymal transition in eukaryotes are a few fundamental processes where any dysregulation or abnormalities in the Notch signaling pathway may lead to several diseases (Fortini 2009). For example, T cell acute lymphoblastic leukemia (T-ALL), Alagille syndrome, spondylocostal dysostosis, Cerebral Autosomal-Dominant Arteriopathy with Subcortical Infarcts and Leukoencephalopathy (CADASIL) syndrome, and aortic valve disease all deal with the abnormal growth or degeneration in the bone or smooth muscle tissues that is contributed to some mutation in Notch signaling components (Artavanis-Tsakonas et al., 1999; Gridley, 2003). Due to the wide range of other developmentally patterned diseases that

are implicated in Notch signaling of vertebrates, Fortini believes that nearly all cells of complex animal tissue may potentially have required Notch signaling for differentiation at some point (2009).

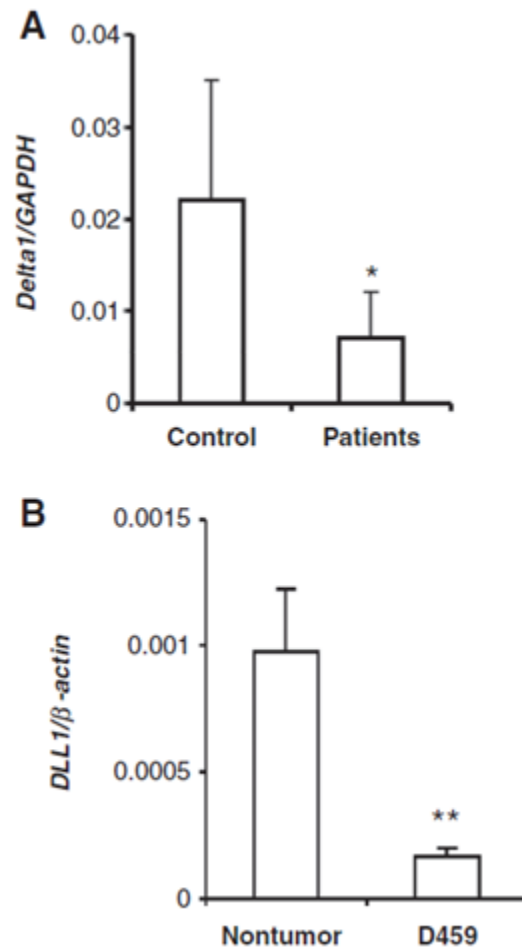


Figure 1 DLL1 expression in human and mice in normal and tumor tissues (Huang 2011)

A prototypal example of cell proliferation and a driving force for research of the Notch signaling pathway is the inhibition of tumor growth in various cancers. Since DLL1 is naturally under-expressed in tumors in mice and humans (see Figure 1), inducing an overexpression of DLLs in these tumors is the route that the Dikov Laboratory chose. A study done by Huang et al. suggests that a soluble multivalent form

of Delta-like Ligand 1 (DLL1) may offer an effective strategy for therapeutic treatment to overcome T-cell immunosuppression associated with tumors and overall suppress tumor growth (2011). However, the DLL1 showed a dose dependency correlation where higher density of DLL1 promoted T-cell development and inhibited B-cell development but lower density of DLL1 promoted both T-cell and B-cell development (Huang et al., 2011). This study from the Dikov Laboratory supports the feasible attainment of researching the polyvalency of the Notch ligand DLL in suppressing cancer and is the collaborative research the Magliery Laboratory intends to build upon. As evident in the numerous affected structures of the human body, understanding the Notch receptor activation and posttranslational processes that regulate Notch activity may prove insightful for comprehending the full dysfunction to cause these diseases.

The Notch signaling pathway is a well-studied process. The Notch receptor is a transmembrane protein that contains an extracellular domain to bind to ligands and an intracellular domain that will depart into the cell's cytoplasm after proteolysis to induce transcription in the nucleus (as seen in Figure 1).

There are two classes of standard Notch ligands: Delta and Serrate/Jagged. The Delta ligand was first found in *Drosophila* and is a member of the DLS (Delta/Serrate/Lag-2) family of ligands (Chillakuri 2012). The homologous Delta-like ligand (DLL-1) is found in vertebrates, namely mice and humans. DLL-1 binds to the N-terminus of the Notch receptor and triggers the proteomic cleavage event that, in return, causes a cascade of chemical reactions that end with the promotion of transcription. In parallel, Jagged-1, another human homolog to the Jagged found in *Drosophila*, is a

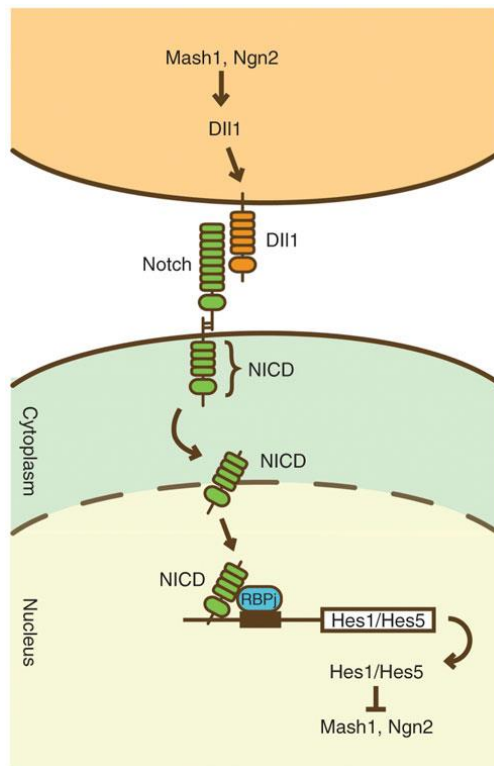


Figure 2 Notch signaling

pathway (Kageyama 2008)

ligand that binds to the Notch receptor has already been more deeply studied for its role in the Notch signaling pathway. Similarly, studying the DLL1 could lead to greater understanding of the immune response tied to the Notch signaling pathway, in particular, with DLL1 binding to Notch receptors and its relevance in cancerous tissues. Due to the transcriptional control that the Notch signaling pathway exerts, it can easily be seen how the deregulation of this system could influence a cell's protein make-up and cell-fate.

It is suggested that the deregulation of the Notch signaling pathway is the cause of many undesirable cellular processes; however, this research will focus on the binding events of the Notch receptors and their influence on cell growth and proliferation in cancer. In the Dikov Laboratory, synthesized aggregates of DLL-1 Notch ligands have shown potential for the therapeutic treatment of cancer. The collaborators in the Dikov

Laboratory have already produced DLL-1 constructs and tested them in mice models in the murine Lewis lung carcinoma (LLC) cell lines for their activity. These aggregates however are heterogenous mixtures and are therefore unsuited for pharmaceutical usage. The Magliery Laboratory is attempting to produce a collection of discrete DLL-1 ligands in order to learn more about the Notch signaling pathway's activation of the Notch receptor.

1.3 FOP Background

The other disease that is believed could be understood better through studying the affected proteins responsible for the disease is FOP. Unlike cancer, FOP is a rarer disease, only affecting one in two million individuals (Pignolo 2013). However, there is no pattern in predisposition in race, ethnicity, gender, or geographic location for the hundreds of individuals diagnosed with classical FOP (Morales-Piga 2010).

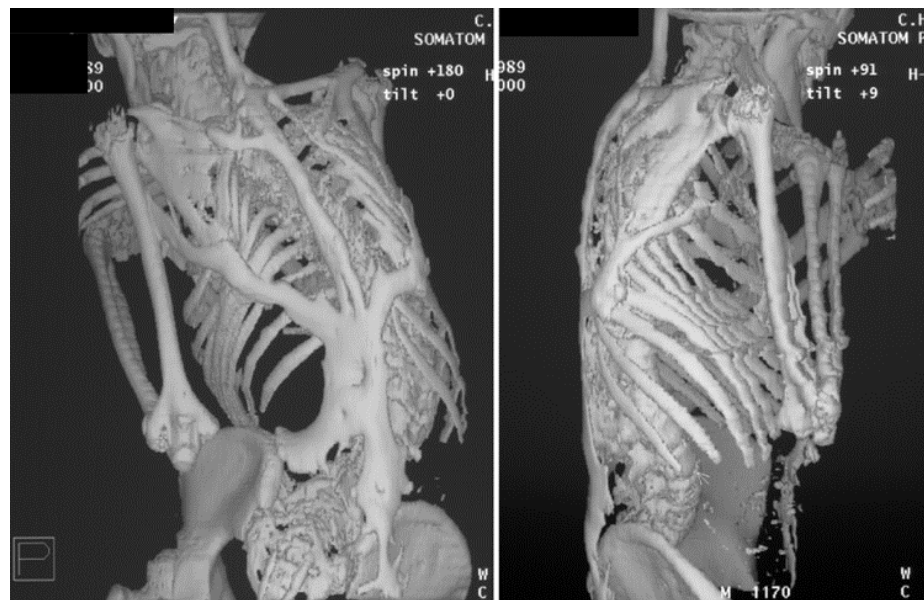


Figure 3 Askeletal bone growth typical in FOP (Glaser 2003)

FOP is distinguished typically by malformations of the hallux and progressive heterotopic endochondral ossification (HEO). FOP is also associated with skeletal anomalies such as clinodactyly malformed thumbs, short femoral necks, and proximal medial tibial osteochondromas (Kaplan 2009). HEO is the nonmalignant overgrowth of bone through the ossification of cartilage by being replaced by real bone tissue. When correctly regulated, this form of bone growth is a normal and essential mechanism in embryonic bone development. However, the ankylosed effects from this HEO disorder accumulate with every episode of injury, wear, and spontaneous flare-up. These painful soft tissue swellings essentially transform ligaments, tendons, aponeuroses, fascia, and skeletal muscles into mature heterotopic bone, leading eventually through the process of endochondral ossification that replaces skeletal muscles and connective tissues with an internal encasement of skeletal bone (Pignolo 2013). The accumulation of this skeletal bone leads to permanent immobility of the individual and eventually causes their death usually due to complications with thoracic insufficiency syndrome where the thorax can no longer support normal respiration and lung function (Campbell 2003). The additive disability of FOP usually leaves patients confined to wheelchairs by their third decade of life and only gives a median age of survival to be approximately 40 years (Kaplan 2005). In efforts to treat this disease, surgery has been tried to remove the excess bone, however this results in an even greater return of bone growth (Pignolo 2013). So, current management focuses on avoiding injury, controlling pain from flare-ups, and optimizing residual function after the episode (Pignolo 2013). In order to obtain a treatment for this

disease that does not increase or worsen the HEO flare-ups, research efforts have been taken up in order to find the source of this disease.

In order to understand more about this disease and how it functions, research at the genetic level reveals the mutation responsible for FOP. A heterozygous point

mutation in the gene encoding for activin receptor type A (ACVR1) on chromosome 2 encodes for a BMP type 1 receptor protein called activin-like kinase 2 (ALK2) that malfunctions and, due to this “gain of function” mutation, causes leaky expression to the BMP signaling pathway (Kaplan 2009). ALK2 (the transmembrane protein is also

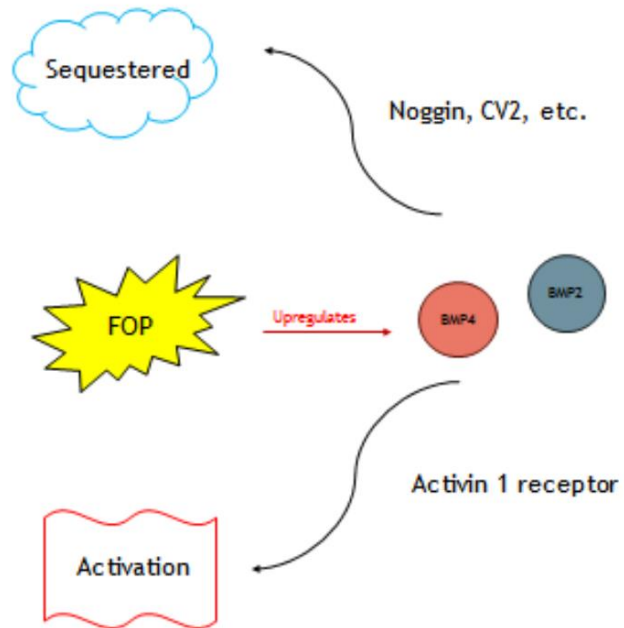


Figure 4 General function of FOP proteins

commonly referenced as ACVR1) is a receptor targeted by BMP growth factors that are responsible for signaling the need for bone growth; however the mutated ACVR1 gene destabilizes a glycine-serine (GS) interaction within the activation domain of ALK2, leading to an intracellular surplus in signaling for bone growth (Shore 2006; Groppe 2007). To augment this problem, BMP4 is specifically over-expressed in classically diagnosed FOP patients, which activates more signaling in lymphoblastoid cells and fibroproliferative cells (Zimmer 2013). The additional bone growth is achieved through the excess signal transmitting to the nucleus via phosphorylation of SMAD signaling

molecules that activates gene transcription (Zimmer 2012). In order to deter overactive intracellular signaling, the body already has a controlling mechanism involving the extracellular antagonist, Noggin (NOG) (Zimmer 2012). In fact, as a high-affinity antagonist of BMP2 and BMP4 that is under-expressed in FOP patients, NOG has been considered as a rational treatment for inhibition BMP4 signal transduction pathways (Glaser 2003). NOG is a secreted homodimeric protein that inhibits the intracellular signal transmission by occluding the binding site on the receptor where BMP would bind (Zimmer 2012). This protein seems like a primary candidate to study in order to determine an approach to an FOP treatment for its inhibitory sequestering effects on the mutated receptor protein. However, studying the BMPs, specifically the ones more commonly related to FOP, BMP2 and BMP4, are also targeted for more in depth research as they are readily antagonized by wild type NOG (Zimmer 2013). With a similar method, a Von Willebrand factor type C domain (VWC) on Crossveinless 2 (CV-2) was determined to be responsible for binding to BMP2 and sequestering the molecule so that BMP2 is incapable of binding to other receptors (Zhang 2008). As a competitive inhibitor, the VWC domain may sequester BMPs, inhibiting their binding to the mutated ACVR1 binding site that causes the over stimulated SMAD pathway indicated as the cause of FOP. In an effort to analyze these proteins and their interactions that are thought to cause FOP, the Magliery lab has decided to produce these proteins for in vitro studies.

1.4 Approaches

1.4.1 Specific to Notch Project

In order to create a discrete polyvalent molecule, the first goal was to create soluble, folded monomers of the DLL1 ligands. Two approaches were taken to accomplish this: attaching a pectate lyase B (pelB) sequence or a Maltose Binding Protein (MBP) domain sequence to the desired protein construct and expressing the unfolded protein then refolding in vitro using an oxido-shuffling system adapted from previous work done on refolding EGF-like domains (Mayhew 1992). Previously, MBP has been successfully used for the soluble overexpression and purification of cysteine-rich proteins, such as crotamine, and was hoped to have a similar success for DLL1 (Thi Vu 2014). In addition to the MBP domain sequence, the sequence for pelB was added to the N-terminal end of DLL1 protein constructs in order to pull the fused protein into the periplasmic space of the gram-negative bacteria *E. coli*. This was done in order to promote a soluble, folded product by the ions and proteins present in this periplasm. The additions of either of these sequences on the DNA level are common techniques in genetic protein engineering. Another goal was to determine which domain of DLL1 was necessary for binding to the notch receptor. Studies of DLL4 suggest that MNNL and EGF domains have specific and essential contact points with the Notch receptor (Luca, 2015). In order to determine more specifically the binding sites through in vitro binding experiments, DLL1 proteins with the additional N-terminal MNNL domain, DSL domain, and two or three EGF domains were cloned, expressed with a pelB leader sequence, and refolded. With the ultimate goal of producing a discrete polyvalent

molecule, a C-terminal cysteine residue was added to the original DSL-EGF-EGF and DSL-EGF-EGF-EGF constructs in order to produce a site for maleimide chemistry for PEGylation experiments. Because it is currently unknown which domains, and more specifically which residues, are responsible for binding the DLL1s to the notch receptor, a future goal of the Magliery lab is to study this interaction for all of the expressed and soluble monomeric DLL1s via in vitro Surface Plasmon Resonance (SPR) binding studies.

1.4.2 Specific to FOP Project

In order to obtain soluble, folded material for binding studies, the first goal of the project required experiments to optimize the expression of each of these constructs. Since the overall goal of this project is to investigate the bindings between each of these FOP related proteins, the Magliery lab would like to collect binding data via SPR and understand the structures of these protein complexes via crystallography. Currently, the binding and structure between BMP2 and these proteins is known but this remains unknown for BMP4. Since BMP4 has been specified as a possible drug target for FOP by NOG, studying the interactions between these proteins will be the first step in comprehending a drug treatment for FOP.

Chapter 2: Materials and Methods

2.1 Cloning

2.1.1 General Polymerase Chain Reactions (PCR) Procedure

The general PCR reaction requires an initial denaturing of the two original DNA strands of the template at 94 °C for 2 min. Then a repeated denaturation at 94 °C for 30 sec, a specific annealing temperature that worked best for each construct cloned based off initial gradient reactions for 30 sec, and an elongation operation at 72 °C for 30 sec. The number of cycles for this repeated process was 25 for all PCRs. To finish the reaction, an additional extension time of 4 min at 72 °C was spent before bringing the temperature of the final product down to 4 °C for storage. The general contents of a PCR reaction requires a template, forward primer, reverse primer, dNTPs, polymerase, and the respective polymerase's buffer. These PCR reactions were preformed with Pfu polymerase unless otherwise specified with the use of Herculase polymerase.

2.1.2 General Ligation Reaction Procedure

The general ligation reaction required identically digested vectors and inserts. Double digests require two specific restriction enzymes and their compatible buffers. For these digestions, NEB Cutsmart or 3.1 Buffer was used because of their compatibility with NdeI, NcoI, and BamHI. All double digests reacted for 4 hr at 37 °C. Based on the concentrations of digested and purified vector and insert, a determined amount of vector and insert is determined for each reaction so that the ligation is between equal molar ratios of both components. Vector negative and insert negative ligation reactions were also done for controls. Each ligation reacted with T4 ligase in T4 ligase buffer at 16 °C

overnight. Ligation reactions (1 µl) were transformed into DH10B(DE3) cells and grown on antibiotic plates (pHLIC has ampicillin resistance gene) at 37 °C. Colonies picked and grown up in small 2YT media cultures and ampicillin overnight at 37 °C in a shaker at 200 RPM. After hitting the stationary phase of E. coli growth, these cultures were purified by DNA miniprep and then analytically digested and sequenced to determine if the correct sequence had been successfully ligated together and free from PCR product mutations. A glycerol stock of each miniprep was made and stored at -80 °C for back up stocks and discarded later if the sequence was determined to be incorrect.

2.1.3 Cloning MBP and PelB-MBP Notch Constructs

PCR were initially set up for creating human and murine constructs with two and three EGF repeats. These PCRs were done with Pfu polymerase. The templates and primers used for these PCRs can be found in the table below:

	MBP Hu12	MBP Mu12
Template	Human123	Murine123
Fwd primer	MBP_HuNOTCH_Fwd ATT ATT ATA CCATGGC GAG AAT CTA TAC TTC CAG	MBP_MuNOTCH_Fwd ATT ATT ATA CCATGGC GAG AAT CTC TAT TTC CAG
Rev primer	Hu12.rev (H) AATAATGGATCCTTACTGGTTA	Mu12.rev (N) AATAATGGATCCTTATTGGTTG CAGAATAAGCC

Table 1 PCR components for insert products for MBP constructs. Reverse primers remain the same form initial construct cloning of huNotch.D12 and muNotch.D12 ordered and used by Dr. Brandon Sullivan

From the pHLIC-MBP plasmid, constructs underwent restriction digestion with NcoI and BamHI enzymes and ligated with the purified and identically digested inserts of Human DSL-EGF1-EGF2, Human DSL-EGF1-EGF2-EGF3, Murine DSL-EGF1-EGF2,

and Murine DSL-EGF1-EGF2-EGF3 that were prepared previously from DLL1 construct containing plasmids.

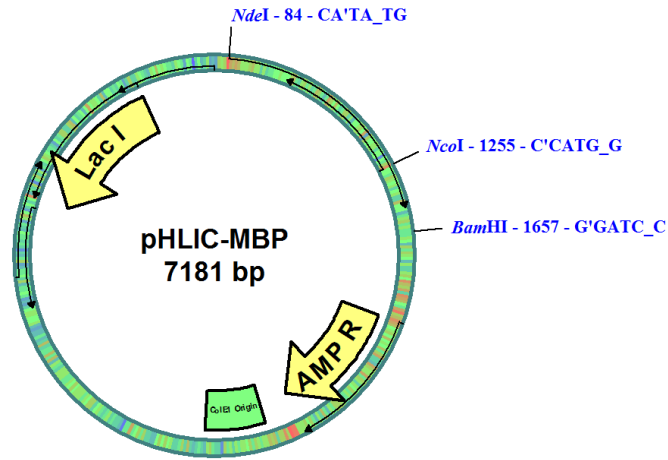


Figure 5 A plasmid map of pHLIC-MBP showing where the restriction enzymes used for cloning, NcoI and BamHI cut into the vector. The NdeI site marks where the MBP domain begins.

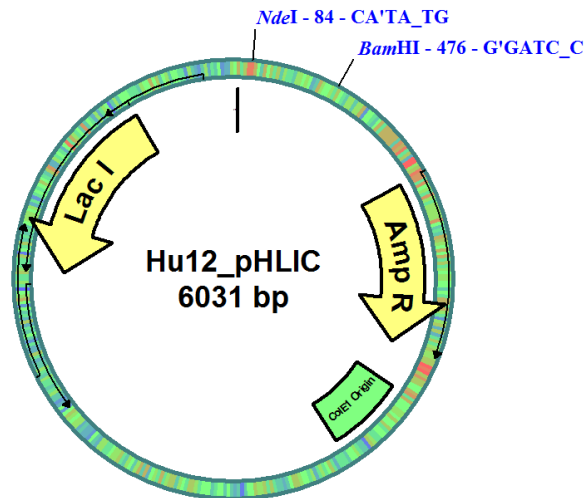


Figure 6 A plasmid map of pHLIC showing where the restriction enzymes used for cloning, NcoI and BamHI cut into the vector to retrieve DLL1 inserts for MBP cloning. This plasmid map contains Hu12 but other plasmids containing Hu123, Mu12, and Mu123 were comparable digestion scheme and set up.

In order to clone PelB-MBP, the PCR product was created using the material described in **Table 2** below. This PCR product was double digested with NdeI and NcoI and ligated with a similarly digested and purified pHLIC-MBP vector.

	MBP to PelB-MBP plasmid vector
Template	pHLIC-MBP insert
Fwd primer	PelMBP_Fwd: ATT ATT ATT CAT ATG AAA TAT CTG TTA CCT ACT GCT GCT GCG GGA CTA CTT TTA TTA GCG GCA CAA CCA GCA ATG GCG GCG CAT CAT CAT CATCATCACATG
Rev primer	PelMBP_Rev: AATAATAATCCATGGCCGAGGTT GTTG

Table 2 PCR components for insert for PelB-MBP constructs

2.1.4 Cloning MNNL Notch Constructs

The HuMNNL123 and MuMNNL123 sequences were ordered in kanamycin resistant pUC57 plasmid and digested with NdeI and BamHI. The insert containing the HuMNNL123 and MuMNNL123 were used for both ligating into a working vector and obtaining a smaller PCR product for HuMNNL12 and MuMNNL12 constructs. Digested and purified HuMNNL123 and MuMNNL123 were ligated into a purified and similarly digested pHLIC vector similar to the one depicted in **Figure 8**. For the PCR of the two smaller constructs, HuMNNL12 and MuMNNL12, the digested HuMNNL123 and MuMNNL123 constructs were used as templates. The PCR for the HuMNNL12 required

Herculase polymerase while the MuMNNL12 has failed to work with either Herculase or Pfu polymerases thus far. The remaining specific contents of each PCR were as follows:

	HuMNNL12 construct	MuMNNL12 construct
Template	HuMNNL123	MuMNNL123
Fwd primer	HuFwdMNNLpel ATTATTCATATGAA ATATCTTCTCCCCAC	MuFwdMNNLpel ATTATTATTCATATG AAATACTTGCTACC
Rev primer	MNNL_Hu12_Rev AATAATGGATCCTT AGTTGCAGAATAGT CCGCCCCAACC	Mu12RevMNNL AATAATAATGGATCCTT AATTGCAAAAAAGGCCCCC

Table 3 PCR Primers for HuMNNL12 and MuMNNL12 Constructs

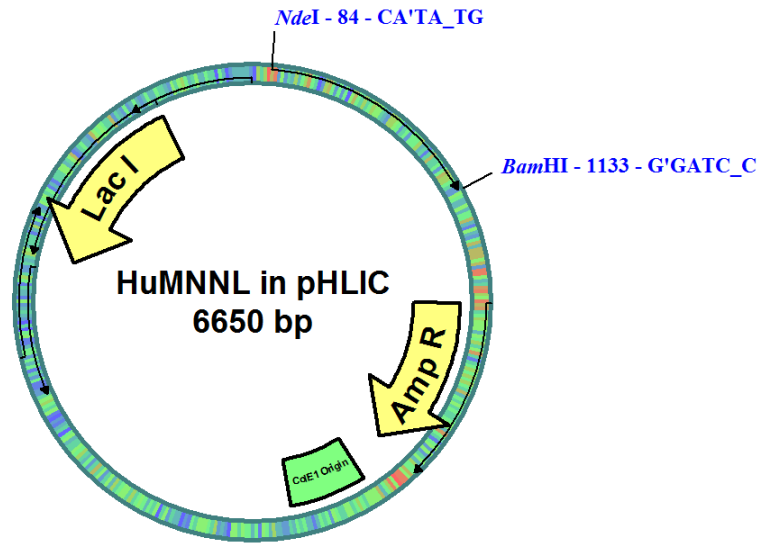


Figure 7 A plasmid map of pHLIC showing where the restriction enzymes used for cloning, NdeI and BamHI cut into the vector to retrieve DLL1 inserts for MNNL cloning. This particular plasmid contains HuMNNL123 but the plasmid containing MuMNNL123 is comparable. After ligation the HuMNNL123 and the MuMNNL123 are replaced with HuMNNL12 and MuMNNL12 on the plasmid map.

2.1.5 Cloning AVCR, VWC, BMP2, BMP4, and Noggin FOP related Constructs

Dr. Nicholas W. Callahan's work on cloning FOP related constructs with a pelB sequence prior to the specific human gene sequence for ACVR, VWC, BMP2, BMP4, and Noggin provided the basis for using restriction digest and ligation reactions alone to achieve different cloning products without the pelB leader sequence. Through digestion with NcoI and BamHI in NEB 3.1 Buffer, the desired gene can be isolated from the plasmid vector with the pelB leader sequence and ligated into a vector without the pelB leader sequence. This allows the expression of this protein that does not initially contain the pelB leader sequence and therefore will not be pulled into the periplasmic region of the E. coli cells during expression. However, the His tag was left on this construct in order to purify it late. To test if the His tag effects the expression of each protein, a construct with no tags was constructed. The untagged construct required a PCR to insert a restriction site between the His tag sequence and the desired gene sequence. This untagged construct was prepared by Dr. Nicholas W. Callahan.

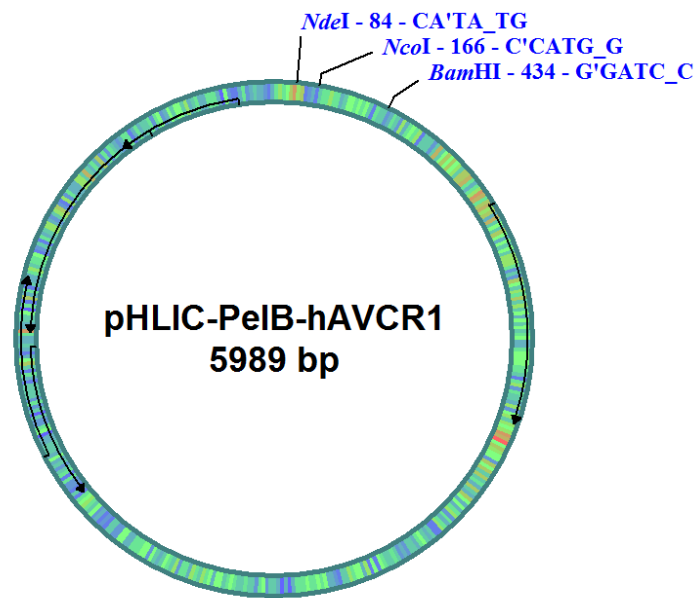


Figure 8 A plasmid map of pHLIC showing where the restriction enzymes used for cloning, NcoI and BamHI, cut into the vector to retrieve desired gene (in this case ACVR) inserts for each FOP related protein. The removed peIB leader sequence is coded for between NdeI and NcoI. For cloning the untagged variant, the NCOI restriction site was moved effectively closer to the BamHI site to remove the His-tag sequence that exists on this example.

2.2 Expression, Lysing, Purification

2.2.1 Expression and Lysing General Protocol

All *E. coli* expressions were completed by transforming the pHLIC plasmid containing the desired gene with T7 overexpression into BL21(DE3), Origami, C41(DE3), and C43(DE3) cells. The transformed cells are plated on LB Agar media plates containing ampicillin and left to incubate at 37 °C overnight. The surviving colonies on the plate were successfully transformed by exhibiting the ampicillin antibiotic resistance gene coded for in the desired pHLIC plasmid. A single colony is picked using flame sterilization and were grown in 2YT media seed cultures of 30 mL with .1 g/L ampicillin overnight. These seed cultures were used to inoculate 1 to 2 L of fresh 2YT media in 4 L flasks with an additional 0.1 g/L ampicillin. Conditions of the lag phase of *E. coli* growth were optimized with temperature adjustments depending on the specific protein constructs, with the employment of baffled or non-baffled flasks, and with or without a cold-shock step of incubating at ~4 °C for 30 min to slow cell growth before induction. After incubating for 2 hrs in a shaker at 200 RPM, the cultures are checked for an OD₆₀₀ between 0.6 and 1.0 before inducing the culture with 0.5 mM IPTG. The cells are then allowed to grow overnight at 16 °C at 120 RPM in the shaker.

The cell are centrifuged at 6000 RPM for 10 min at 4 °C. After decanting the supernatant, the pellets were re-suspended with 25 mL of lysis buffer (50 mM Tris-HCl, 300 mM NaCl, 10 mM imidazole, pH 8) per liter of culture from which the pellet was secured. In addition, 5 mM MgCl₂, 0.5 mM CaCl₂, 5 µl of DNase and RNase (at 5 mg/mL each) per liter of culture pelleted, 0.1% Triton X-100, and 25 mg of lysozyme

(per liter of culture pelleted). The mixture was nutated for 10 min at 4 °C or allowed to sit on ice with occasional agitation for 10 min. The cells were then lysed via glass beads, sonication, or Emulsiflex. When lysing with glass beads, 0.1 mm glass beads (~0.5 mL per liter of culture pelleted) were vortexed for a total of 10 minutes in the re-suspended pellet mixture. When performing the sonication lysing method, the mixture on ice was pulsed with an amplitude of 6 for 30 seconds every minute for a total of 6 pulses. When utilizing the Emulsiflex instrument, the pellet mixture was kept on ice between three cycles through the instrument with a pressure differential between 15,000 and 20,000 psi before being flushed out with lysis buffer. Once the lysate obtained a homogenous consistency, it was centrifuged for 45 minutes to an hour at 15,000 RPM to 17,000 RPM at 4 °C. Depending on the protein expressed, the purification methods were adapted appropriately.

2.2.2 Notch Protein Expression and Purification Protocols: Variants of Hu and Mu

D12(3)

Construct	Strain	Description	MW (kDa)
35	huNotch.pD123	Human PelB-His6-TEV-DSL-EGF1-EGF2-EGF3	20.9
36	huNotch.D123	Human His6-TEV-DSL-EGF1-EGF2-EGF3	18.7
37	huNotch.D12	Human His6-TEV-DSL-EGF1-EGF2	14.3
38	huNotch.pD12	Human PelB-His6-TEV-DSL-EGF1-EGF2	16.6
39	muNotch.D123	Murine His6-TEV-DSL-EGF1-EGF2-EGF3	18.7
40	muNotch.pD123	Murine PelB-His6-TEV-DSL-EGF1-EGF2-EGF3	20.9
41	muNotch.pD12	Murine PelB-His6-TEV-DSL-EGF1-EGF2	16.6
42	muNotch.D12	Murine His6-TEV-DSL-EGF1-EGF2	14.3

44	MBPhuNotch.D12	Human MBP – TEV – DSL – EGF 1 – EGF 2	57.3
45	MBPhuNotch.D123	Human MBP – TEV – DSL – EGF 1 – EGF 2 – EGF3	61.7
46	MBPmuNotch.D12	Murine MBP – TEV – DSL – EGF 1 – EGF 2	57.3
47	MBPmuNotch.D123	Murine MBP – TEV – DSL – EGF 1 – EGF 2 – EGF3	61.7
48	pelMBPhuNotch.12	Human pelB-His6 -MBP-TEV-DSL-EGF1-EGF2	59.6
50	huNotch.D123C	His6-TEV-DSL-EGF1-EGF2-EGF3-Cys	19.1
52	huNotch.D12C	His6-TEV-DSL-EGF1-EGF2-Cys	14.7
57	huNotch.pMD123	Human pelB-His6 -TEV-MNNL-DSL-EGF1-EGF2-EGF3	36.1
58	muNotch.pMD123	Murine pelB-His6 -TEV-MNNL-DSL-EGF1-EGF2-EGF3	34.7
80	huNotch.pMD12	Human pelB-His6 -TEV-MNNL-DSL-EGF1-EGF2	34.0

Table 4 DLL1 Construct Variants

For both human and murine protein constructs, the respectively gene coded plasmid was transformed into C43 (DE3) or Origami (DE3) cells. During lag phase, the cultures were incubated at 37 °C in non-baffled flasks. Initially, the culture was then cold-shocked for 40 minutes in the cold room at 4 °C but in later modifications to the protocol, this step was determined to have little effect on yield and removed. After inoculating with IPTG, the expression was allowed to proceed for 6 hours to overnight.

Several lysing options were used in order to obtain and purify the desired protein. Following the glass bead lysis method, the lysate was centrifuged at 17,000 RPM at 4 °C for 30 minutes. The supernatant was re-centrifuged in the same way to ensure only soluble product was in the sample. This supernatant was mutated with 1 mL Ni-NTA 50% slurry or Amylose 80% slurry per liter of culture for 30 min in the cold room at 4 °C. When the supernatant was determined to not contain the desired protein product,

larger cultures were grown and lysed following the emulsiflex protocol. The lysate was similarly centrifuged but the pellet containing the aggregated desired protein was kept. These samples underwent harsh conditions in the unfolding buffer (5 M Guanidine HCl, 50 mM Tris-HCl, 50 mM NaCl) overnight in a 200 RPM shaker at 37 °C. The sample was centrifuged at 17,000 RPM at 4 °C for 30 minutes and the supernatant was then refolded through an oxido-shuffling system (100 mM Tris, 0.3 mM cystine, 3 mM cysteine, 1 mM EDTA) through dialysis in the cold room at 4 °C in 4 hour increments until ~0 M Guanidine HCl was achieved. This method was later shortened and adapted to be done with washes (2 M, 1.5 M, 1 M, 0.5 M, 0.25 M, 0.125 M, 0 M unfolding buffer series of washes) directly on a Ni-NTA column. Columns were run initially at 4 °C in the cold room then modified to be run at 37 °C. Flow through, wash buffer (50 mM Tris-HCl, 300 mM NaCl, 20 mM imidazole) at 2 mL per liter of culture, and elution buffer (50 mM Tris-HCl, 300 mM NaCl, 250 - 300 mM imidazole or 1 mM maltose) 3 mL per liter of culture were collected to observe on SDS-PAGE gels.

Collected samples containing the desired protein were then dialyzed into lysis buffer. Once in lysis buffer, the sample was TEV cleaved at room temperature with 100 µl of TEV protease twice for over 6 hours increments in the presence of 5 mM DTT to verify identity and obtain the desired untagged protein for assays and analysis. To further prepare samples for collaborators, the samples were dialyzed into PBS buffer (8 g NaCl, 0.2 g KCl, 1.44 g NaHPO₄, 0.24 g KH₂PO₄ in 1 L 18 MΩ-cm water, pH 7.2).

2.2.3 FOP Related Protein Expression: Optimization between BL21 (DE3) and C41 (DE3) cell lines

Constructs Name	Description	MW (kDa)
hNoggin	No Tag	23.05
hVWC1	No Tag	7.33
hBMP2	No Tag	12.91
hBMP4	No Tag	13.13
hACVR1	No Tag	8.75
His-hNoggin	His Tag	25.19
His-hVWC1	His Tag	9.38
His-hBMP2	His Tag	15.07
His-hBMP4	His Tag	15.29
His-hACVR1	His Tag	10.91
PelB-His-hNoggin	PelB-His Tag	27.37
PelB-His-hVWC1	PelB-His Tag	11.65
PelB-His-hBMP2	PelB-His Tag	17.23
PelB-His-hBMP4	PelB-His Tag	17.45
PelB-His-hACVR1	PelB-His Tag	13.07

Table 5 FOP related variants and their molecular weights

All five FOP related constructs, ACVR1, BMP2, BMP4, VWC, and Noggin, were transformed into BL21 cell line and grown in 1 L batches of 2YT media in non-baffled flasks as the general protocol dictates without a cold-shock step. After centrifugation, the pellets were lysed via sonification after re-suspension in 25 mL of unfolding buffer (6 M Guanidine HCl, 20 mM Sodium phosphate, 500 mM NaCl at pH 7.8). The sonicated sample was then incubated with 1 mM BME in a 200 RPM shaker at 37 °C for 4 hours.

The samples were spun down at 15,000 RPM for 30 minutes at 4 °C. The supernatant was then bound with 1 mL Ni-NTA 50% slurry per liter of grown culture and incubated overnight at 4 °C on a nutator. Each sample on a column was washed with 10 mL of urea wash buffer (8 M urea, 20 mM Sodium Phosphate, 500 mM NaCl, at pH6) and eluted with 10 mL of urea elution buffer (8 M urea, 20 mM sodium phosphate, 500 mM NaCl, at pH 4). Collected samples were run on an 18% SDS-PAGE gel for analysis.

2.2.4 FOP Related Protein Expression: Optimization among PelB-His Tagged, His Tagged, and Untagged

In collaborative efforts with Dr. Nicholas W. Callahan, three variants, PelB-His tagged, His-tagged, and untagged, were cloned in pHLIC and ready for transformation. Plasmids containing ACVR and VWC were transformed into C41 (DE3) and plasmids containing BMP2, BMP4, and Noggin were transformed into BL21 (DE3) as these were determined the best cell lines for expression. For controls, BL21 (DE3) and C41 (DE3) cells that did not undergo transformation were also prepped the following way for expression. As these were a small scale expression experiments, only 1 mL of culture was grown up in 2YT media with 0.1 mg/mL of ampicillin and incubated overnight at 37 °C in a shaker at 200 RPM. After reaching a saturated state, 100 µl of the saturated sample was mixed with 0.1 mg/mL ampicillin in 900 µl of 2YT media and 100 µl of the saturated sample was mixed with 100 µM IPTG and 1 mM ampicillin in 900µl of 2YT media so that each variant construct had a replicate grown in exactly the same manner thus far as a control. With the 100 µM IPTG to induce overexpression, the culture was allowed to incubate at 37 °C in a shaker at 200 RPM for 4 hours. These 1 mL cultures

were centrifuged at 13,000 RPM at 4 °C for 10 minutes and the supernatant decanted and discarded. The pellet, containing the desired protein, was combined with (0.5 µL) 0.1 mm glass beads and re-suspended directly with 200 µl of SDS-loading Buffer via vortex for 4 min for each sample. Samples were heated at 95 °C for 10 min for complete denaturation to be ran on an SDS-PAGE gel.

2.3 Conjugation

2.3.1 Notch C-terminal Cysteine Conjugation Experiments

For post-TEV cleaved Notch human constructs following the structure of DSL-EGF1-EGF2(-EGF3)-Cys, several protocols were followed in order to optimize C-terminal cysteine PEGylation via maleimide chemistry. Samples were dialyzed into either PBS buffer (at pH 7 or pH 8) or lysis buffer (with 10% glycerol, at pH 6) to react with PEG solution. Stock PEG solutions were made fresh before each experiment and varied in concentration due to calculations based on varying protein concentration approximations. The ratio of PEG to targeted protein, the temperature of the reaction, and the time allotted for the reaction were controlled variables for each reaction.

Due to observing massive over-PEGylation in data priorly collected by Nicholas Emerson Long, the first attempt at PEGylation was done at ratios 0.25x, 0.5x, and 1x of PEG (20 kDa) to protein in the hopes of a lower PEG concentration would lead to more selective cysteine binding. This reaction took place in PBS buffer at pH 7 for 1.5 hours at room temperature. The reaction was quenched at 4 °C.

The second attempt at PEGylation was done at room temperature overnight with ratios 5x, 10x, and 20x of PEG to protein in both PBS buffer at pH8 and lysis buffer (with 10% glycerol at pH6) with 0.1 mM TCEP to free terminal cysteines from dimer formation. The reaction was quenched by placing in the fridge at 4 °C.

2.4 Analysis

2.4.1 Western Blot

A 12.5% SDS-PAGE gel was run with the loaded denatured proteins at 180 V for one hour. The proteins of the gel was transferred to nitrocellulose paper (HyBond ECL from GE Amersham) in a transfer buffer (10% methanol, 25 mM Tris, 192 mM glycine) at 200 V for 1 hour and 20 minutes. The membrane was washed five times with PBST buffer (0.05% Tween, 8 g NaCl, 0.2 g KCl, 1.44 g NaHPO₄, 0.24 g KH₂PO₄ in 1 L 18 MΩ-cm water, pH 7.2) and then blocked overnight by incubating the nitrocellulose with 5% Bovine Serum Albumin (BSA) at 4 °C. Once the nitrocellulose was blocked for any non-specific binding to the membrane, the nitrocellulose was washed with PBST buffer three times. The primary antibody (anti-His6-antibody) was diluted in PBS buffer and allowed to bind to the specific His6 tag on the desired protein through nutation overnight at 4 °C. The nitrocellulose was washed with PBST buffer five times in 50 mL quantities to remove excess primary antibody. After washing, a diaminobenzidine (DAB) solution (1 mg/mL diaminobenzidine in 50 mM Tris, pH 7.2) and a hydrogen peroxide (H₂O₂) solution (0.02% H₂O₂ in PBS buffer) was simultaneously added in equal parts to the

washed nitrocellulose in order to develop the membrane. On the developing membrane, a brown precipitate formed overtime, indicating the histidine tag on the desired proteins.

2.4.2 Matrix-Assisted Laser Desorption/Ionization Time-of-Flight Mass Spectrometry (MALDI-TOF MS)

Protein samples were mixed with an equal sample of the prepped MALDI matrix (0.05% TFA, 50% acetonitrile, sinapinic acid). The matrix-protein mixture of each sample was loaded in volumes of 1 μ L to 1.5 μ L onto a clean and dry MALDI plate and was then allowed to dry for several hours. Using the Bruker microflex MALDI-TOF MS, graduate student Sidharth Mohan operated and collected the data from each sample.

Chapter 3: Results and Discussion

3.1 Notch Project - Cloning, Expression, purification, and refolding of Notch constructs

3.1.1 Human and Murine (*PelB*)-His-DSL-EGF1-EGF2-(EGF3)

The desired expressed proteins were determined to be insoluble and in the pellet after lysing the cells. As seen by the double band in the pellets of the expression, the constructs with the *PelB* leader sequence seemed to not cleave by a signal peptidase in the periplasm of the bacteria to cleave off the histidine tag per its normal function. The bigger band for these constructs seems to still have the *pelB* protein sequence attached to the construct, which could lead to messier purification later with two His-tagged constructs close in size. Also if the *pelB* sequence did not successively pull the protein into the periplasm to be folded and in the soluble fraction, but instead the desired protein aggregates inside the cell during expression, a new strategy would have to be used to obtain our samples in the supernatant. It was interesting to see a different protein of a comparable size to the notch constructs being expressed but not sticking to the Ni-NTA column. We initially doubted this was the desired proteins because they contained the His-tag that would bind it to the nickel and should not have ran off the column until the elution. To ensure that our interpretations of these gels were correct, a Western Blot was run from a new gel containing just the pellets of our lysate.

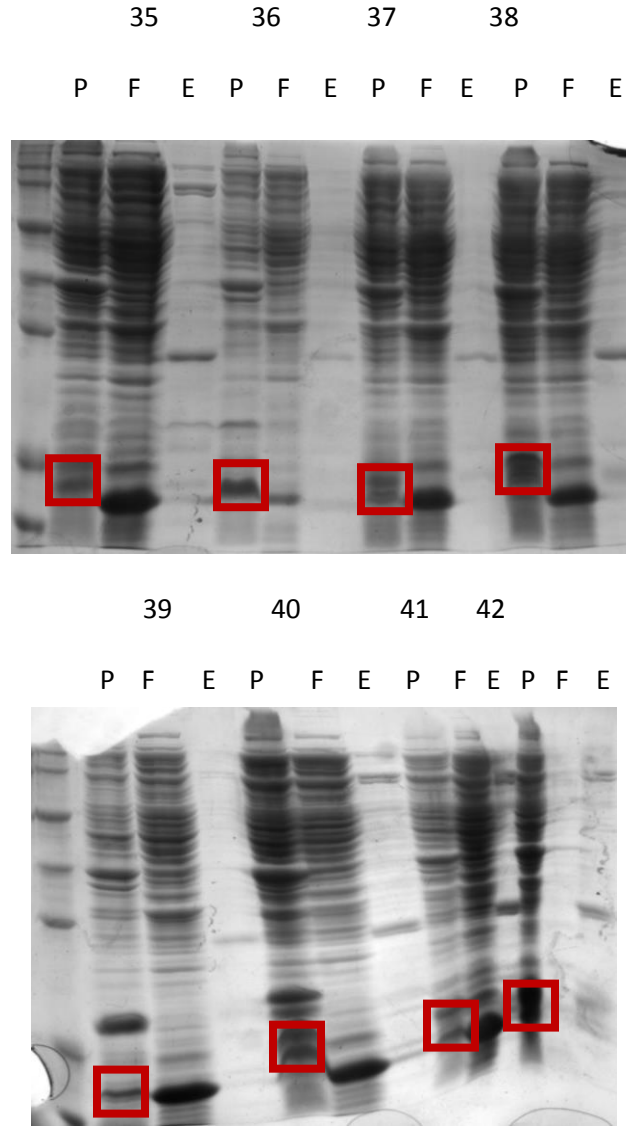


Figure 9 12.5% SDS-PAGE gels comparing expression of human and murine constructs with and without pelB leader sequence.

As this was the first time expressing these proteins and due to the mess of the pellets on the 12.5% SDS-PAGE gel, a Western Blot was used to detect the presence of the N-terminal His tag on the constructs. The anti-His6-antibody bound to the His-tagged proteins and was visualized as an insoluble brown color on the nitrocellulose by 3,3'-Diaminobenzidine (DAB). This is due to the conjugated Horseradish Peroxidase (HRP) to the primary antibody that catalyzes chromogenic substrates like DAB to obtain a visual

signal. Other bands were present on the gel that suggests that these are co-expressed proteins that contain a high number of histidines that were also bound to by the anti-His6-antibody.

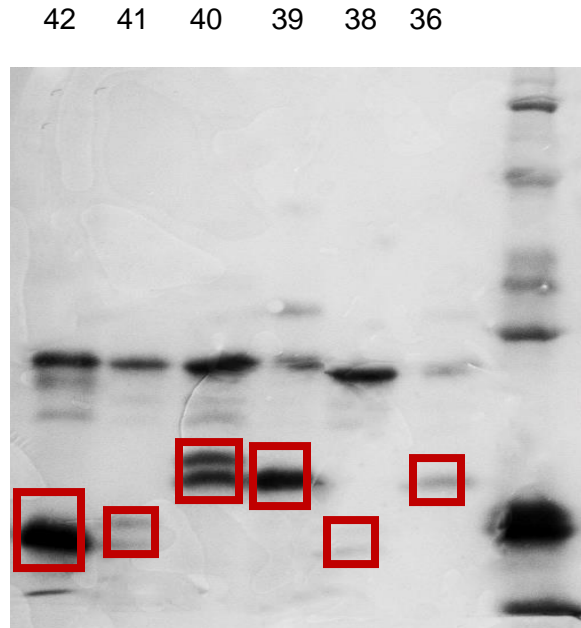


Figure 10 Wesern Blot confirming via an anti-His6 conjugated with HRP that the pellet expression of human and murine constructs with and without pelB leader sequence.

Confirming that the desired DLL1 ligands were being expressed in an insoluble and unfolded manner, several solution pathways presented themselves. One pathway was to clone an MBP tag to the His tagged DLL1 ligands. MBP is a well-behaved and well-folded protein that when attached to another protein, the MBP tag would hopefully pull the proteins into the soluble fraction in the cell. This would mean that the protein would be found in the supernatant of the centrifuged lysate and would be in a folded condition that is needed for further assays by our collaborators. The other pathway was to take these expressions without the pelB sequence in the lysate pellet and re-fold them directly. The re-folding experiments were tested with new expression preps of the murine DLL1

constructs without the pelB leader sequence due to their better expression concentrations as seen on the Western blot (Figure 10). The pellets were re-suspended in a denaturing buffer (5 M guanidine hydrochloride, 50 mM Tris, and 50 mM NaCl). The unfolded DLL1 ligands were solubilized and were found in the supernatant after centrifugation. The supernatant was systematically dialyzed at 4 °C into the oxido-shuffling buffer (5 M, 2.5 M, and 0 M of the denaturing buffer) containing EDTA, 0.1 M cysteine, and 0.5 M cystine. As seen in the 12.5% SDS-PAGE gel (Figure 11), a portion of the desired DLL1 ligands were soluble in the elutions but much more of the desired protein precipitated in the re-folding buffer.

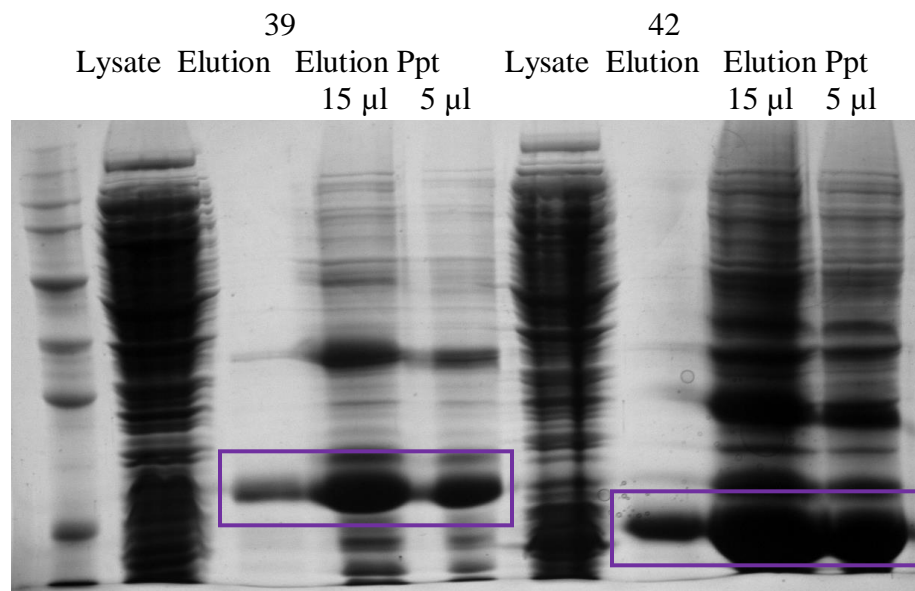


Figure 11 12.5% SDS-PAGE gels comparing soluble elution vs elution precipitate after re-folding experiment for muNotch.D123 and muNotch.D12, respectively.

For purification, the now soluble protein found in the elution was then TEV

cleaved and ran on a Ni-NTA column. The TEV cleaved protein lacks the His-tag and therefore is found in the flow through fraction of the sample collected from the column

and runs farther on SDS-PAGE gels. This common technique for purification was then applied to future expressions of proteins.

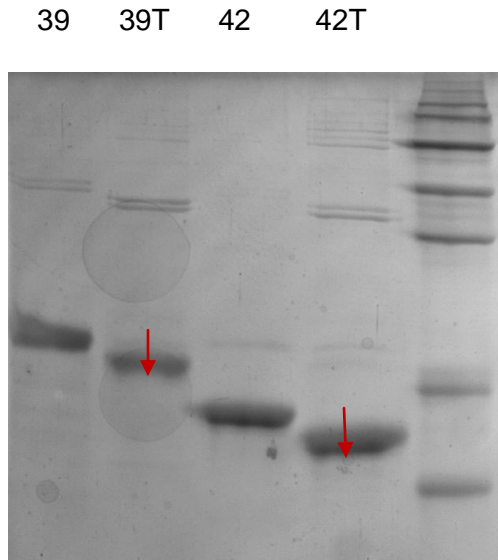


Figure 12 12.5% SDS-PAGE gels comparing pre-and post-TEV cleavage samples of for muNotch.D123 and muNotch.D12, respectively.

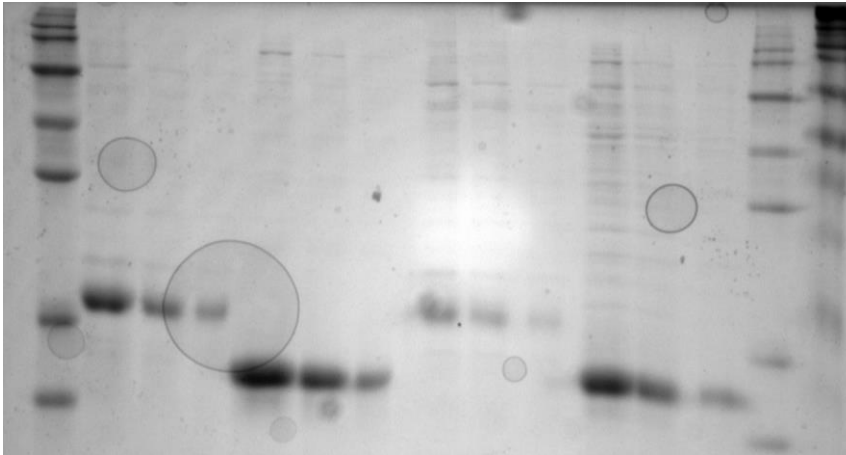
All of the constructs described by the His-TEV-DSL-EGF1-EGF2-(EGF3) were re-expressed, re-folded, and TEV-cleaved successfully using this same method (Figure 12). These sample were prepped for our collaborators with the Dikov laboratory in PBS buffer for their assays.

36

37

39

42



Concentration Estimations:	
36 – Hu 1-3	0.4 mg/mL
37 – Hu 1-2	0.8 mg/mL
39 – Mu 1-3	0.1 mg/mL
42 – Mu 1-2	0.4 mg/mL

Figure 13 Samples prepped for Dikov laboratory collaborators. Concentrations Determined from three different amounts loaded on the gel (10 μ l, 5 μ l, and 2.5 μ l, respectively)

Though this method worked for folding the DLL1s from the pellets, it was an intensive process that is not easily replicated in large batches. If the expressed protein was already soluble, the whole re-folding process would be removed and less product would be lost due to this step. Attempting to express these four constructs in Origami cells, which are known for containing a more oxidized environment that allow the cysteine residues to create disulfides more easily and fold proteins like DLL1 with many cysteine residues, proved unsuccessful as these DLL1s were expressed in the pellet as well.

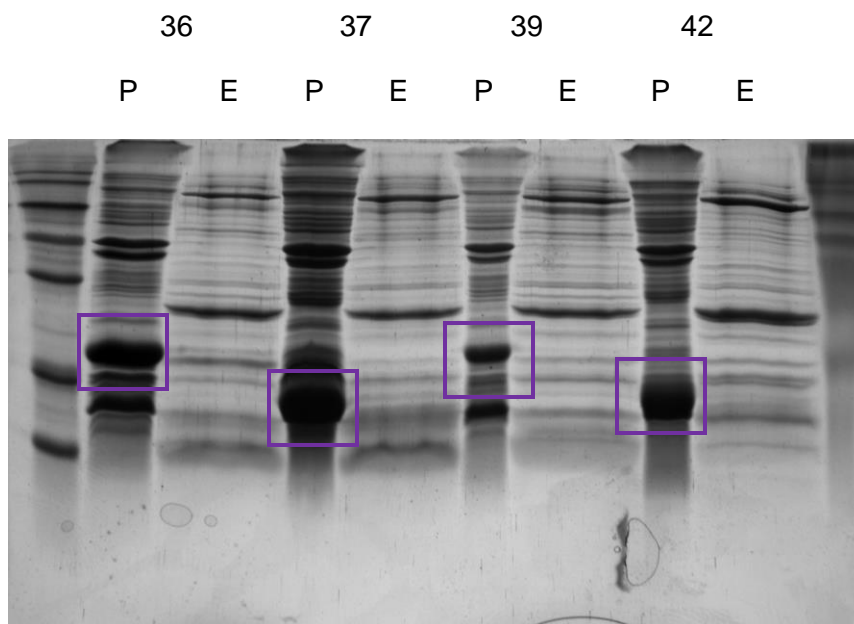


Figure 14 DLL1 variants expressed in Origami cells

3.1.2 Human and Murine (*PelB*)-MBP-*His*-TEV-*DSL*-EGF1-EGF2-(EGF3)

In order to pull the desired protein into the soluble fraction of the expression in a naturally folded way to avoid the re-folding process from the pellet, initially the idea to add an MBP tag to the beginning of the sequence would have this desired effect. Yet, the initial constructs possessed a *PelB* leader sequence that could pull the protein to fold in the periplasm that has natural proteins that help the creation of disulfide bonds in its reducing environment. So this *PelB* leader sequence was also cloned onto the MBP constructs and expression was compared in the C43 (DE3) cell line, in which the original constructs that lacked any MBP tag was proven to express best.

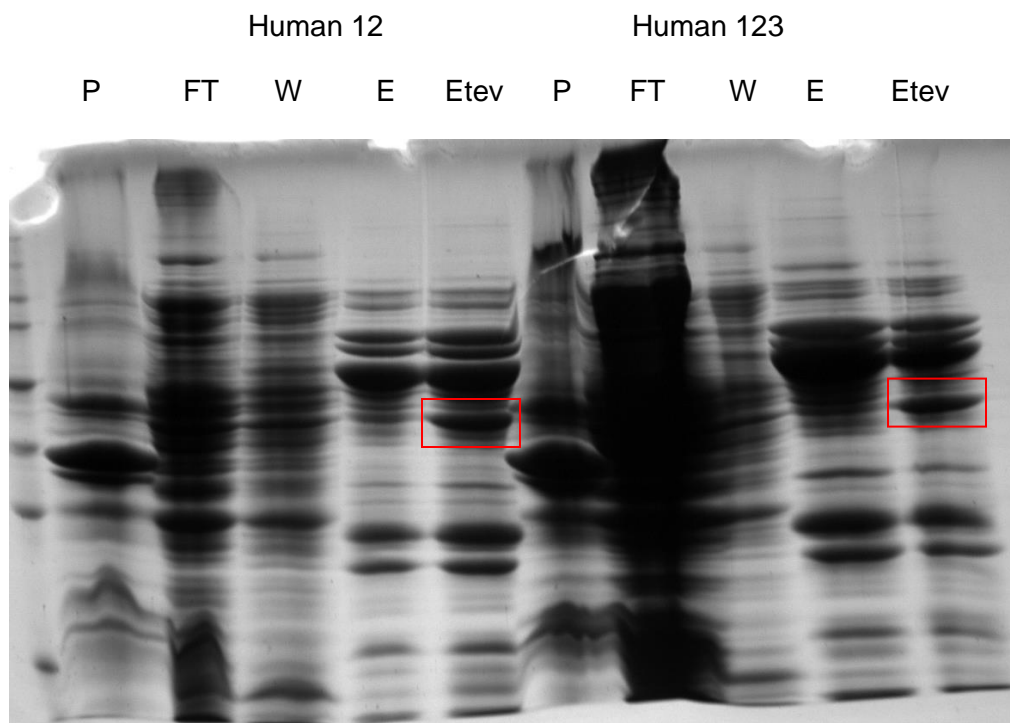


Figure 15 1st nickel column and TEV-cleaved product (only depicts human constructs)

After TEV cleavage, the appearance of just MBP with no DLL1 protein attached is seen on the gel in the red box. This hopefully means that our protein was expressed in the soluble fraction but our protein could have aggregated or may be the same size as another protein in the mess at the bottom of the gel. To clean up the sample, a second Ni-NTA column was ran with the TEV-cleaved elution sample (Figure 16). However, the flow through did not seem to contain much protein the size of the DLL1 proteins and it was speculated that during TEV-cleavage, the DLL1s aggregated and precipitated out of solution.

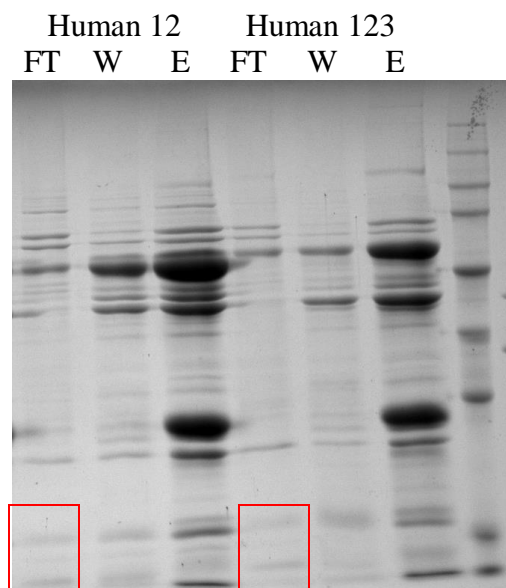


Figure 16 2nd nickel column of Human constructs

Continuing in the efforts towards a soluble DLL1 protein expression, a PelB-MBP tag was constructed via PCR and ligated into the pHLIC-MBP vector containing human DLL1 with two EGF domains (see protocol 2.1.3). Once the cloning of the PelB-MBP construct for the human DLL1 with two EGF domains was sequenced by Genewiz and deemed successful, the MBP tag and the PelB-MBP tag were compared for expression in C43 cell line. In order to better follow where the DLL1 proteins ended up after TEV-cleavage, both a Ni-NTA column and Amylose column were run.

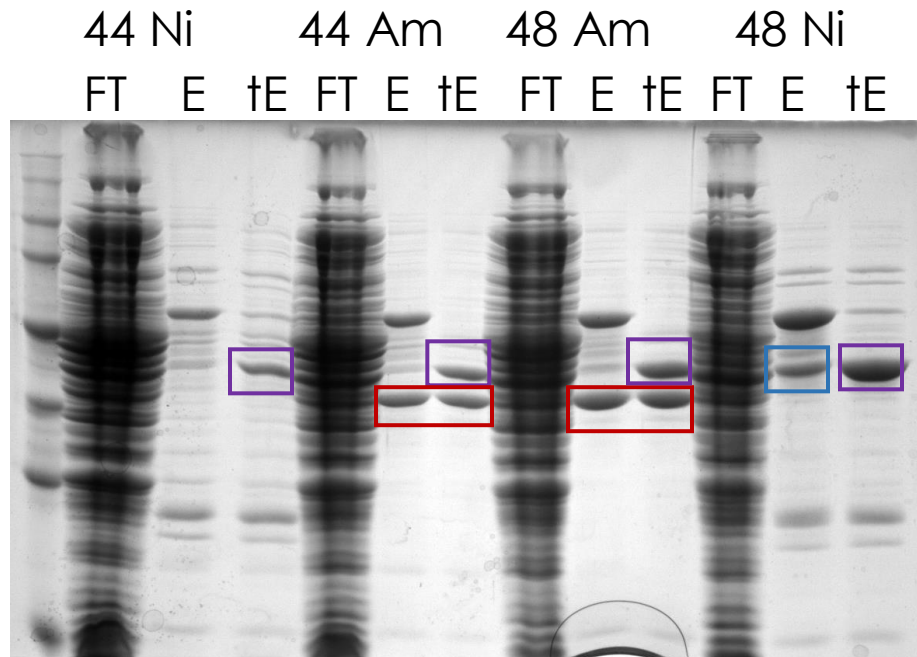
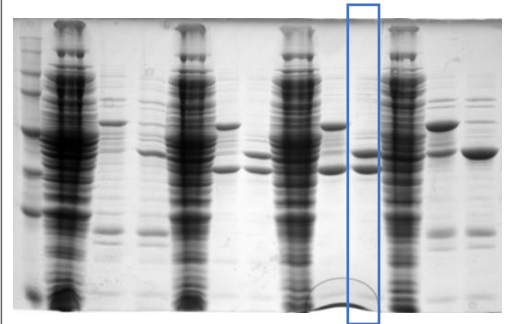
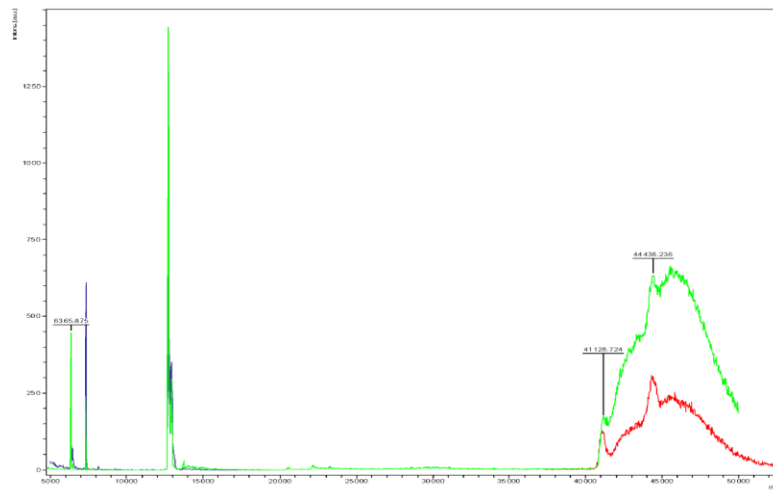


Figure 17 Ni-NTA column and Amylose column for each sample

On the 12.5% SDS-PAGE gel, MBP can be seen to cleave off in both TEV cleaved elutions (purple). However, in the amylose columns it is seen that MBP could be unintentionally cleaving in an unpredicted location (red) that does not contain the His-tag and would otherwise not have been found without the amylose column. There may also be unintentional cleaving near the anticipated TEV-cleavage site as shown in the elution column for the PelB-MBP Hu12 construct that had not yet been TEV cleaved (blue). Regardless, the outcome of where the desired DLL1 proteins are is unpredictable from this gel. So in order to determine if the DLL1 proteins were still in the TEV cleaved elutions, MALDI mass spectrum was performed on the TEV cleaved fractions. The samples ran from the nickel columns were unsuccessful in receiving information from the MALDI instrument.

Green – 48 Amylose



Blue and Red – 44 Amylose

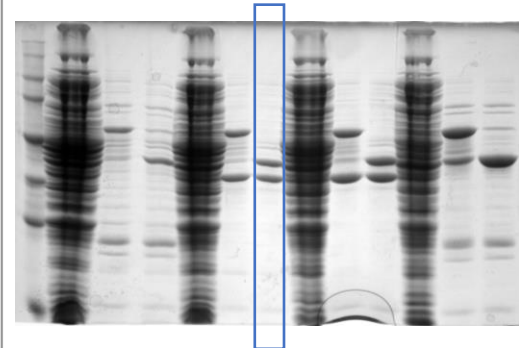
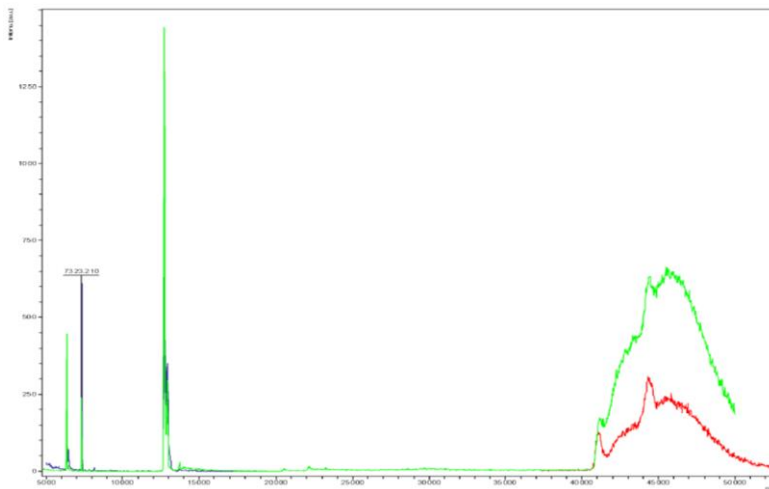


Figure 18 MALDI run on TEV-cleaved elution samples from Amylose column for pelMBPhuNotch.12 and MBPhuNotch.12, respectively.

The peaks on the far right are the bigger MBP proteins while on the left is indicative of the smaller DLL1 constructs existing in the TEV-cleaved elutions for both the PelB-MBP tagged and the MBP-tagged human DLL1 constructs with two EGF

domains. However, because the DLL1 was not seen on the gel, it appears that the DLL1 construct has aggregated and is no longer soluble after Tev-cleavage.

3.1.3 Human and Murine His-TEV-MNNL-DSL-EGF1-EGF2-EGF3 constructs

Initially, expressing the truncated DLL1s without the MNNL domains was thought to be the easier starting point for expression and binding analysis, but as MNNL was thought as a more important domain in the DLL1 constructs for the receptor binding, the project shifted to include this domain. As the MNNL domain is the largest domain of the DLL1 constructs and had to be ordered separately with three EGF domains. The gene constructs had to be digested out of the plasmids that they came in and ligated into pHLIC plasmids or used as PCR templates to create the DLL1 constructs with MNNL and two EGF domains. Creating the smaller DLL1 constructs were especially difficult due to the template size and polymerase ability in the PCR reactions. As the smaller MNNL constructs took more time to compose, expressions of the larger MNNL constructs were conducted in C43 (DE3) cells. Comparable to the DLL1s lacking the MNNL domains, these were still only found to mostly express in the pellet. Even when TEV cleaving the flow through of the supernatants, there was no distinguishable size change on the gel that would indicate this sized band was the correct protein.

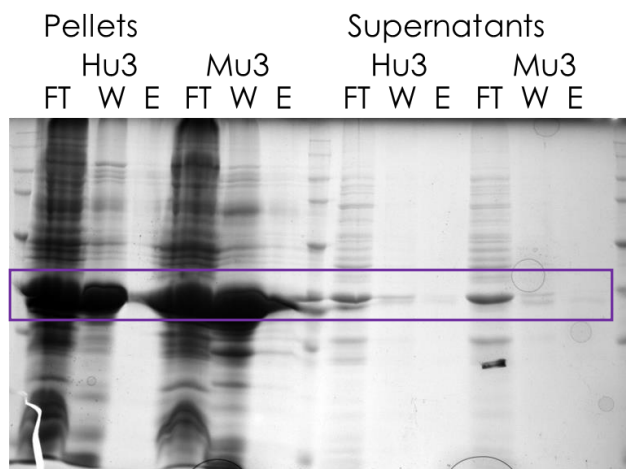


Figure 19 Initial MNNL expression in C43 cells

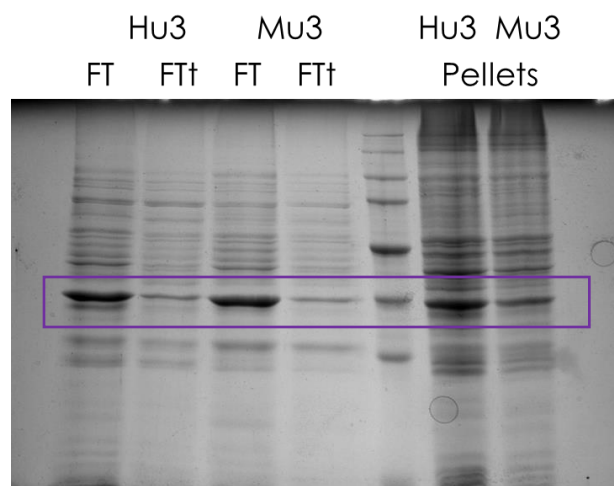


Figure 20 TEV-cleaving MNNL DLL1 constructs from flow through of the supernatant seen in Figure 18.

Through re-folding pellets from the subsequent batches of MNNL containing DLL1s, a soluble and folded product could be obtained. In the future, this construct along with the smaller MNNL containing DLL1s will be used for binding studies and assays by our collaborators in Dikov's lab.

3.1.4 Conjugation of Notch C-terminal Cysteine Constructs

Constructs with a C-terminal cysteine were constructed via PCR modification of the DSL-EGF1-EGF2-(EGF3) constructs for murine and human. The end cysteine residue was added in order to be open for maleimide chemistry for conjugation. Initial PEGylation experiments were done with the huNotch.D123C construct and a 20 kDa PEG molecule but were unsuccessful in showing distinct PEGylation sizes of our desired protein. Further optimization was needed for this reaction. One optimization effort was towards determining the buffer conditions necessary for PEGylation. Literature reports that maleimide chemistry works best at a pH between 5.5 and 7.5. However, our protein has been known to precipitate out of solution at lower pHs and high concentrations of salt during the conjugation reaction. An attempt at solving this precipitation problem was imposed by using a buffer with glycerol that retains a similar pH and salt concentration that the storage elution buffer exhibits. Also, since literature reports that maleimide chemistry works best at a pH between 5.5 and 7.5 and previous PEGylations done in our lab notice more selectivity on the lower end of this range, a conjugation reaction in PBS buffer at pH 6 was performed. From the PEGylation reaction, there was a notably smaller amount of precipitation in the pH 8 buffer than that in the lower pH buffer. However, it seems that there was over-PEGylation in every reaction.

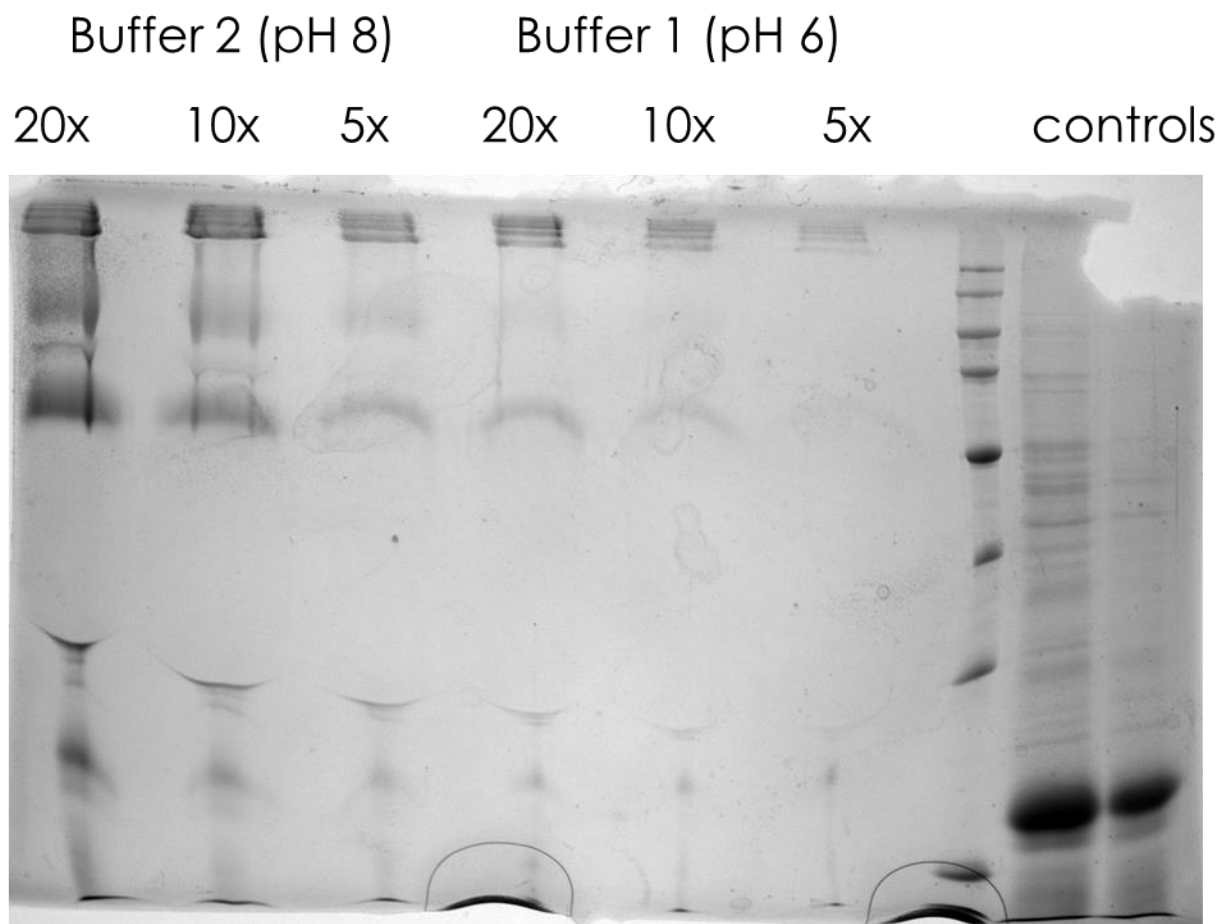


Figure 21 Over-PEGylated huNotch.D123C

In the future, the optimization of this PEGylation reaction will be crucial when crosslinking these DLL1s through multi-conjugation molecules. If these conjugations with multiple monomers are successful, the creation of a discrete, polyvalent molecule could be created and assessed by our collaborators.

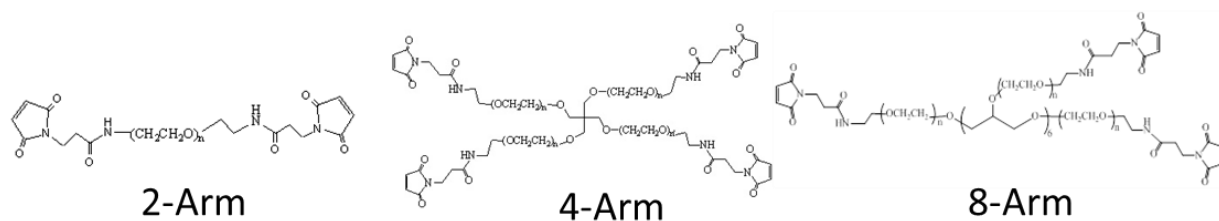


Figure 22 Future PEG molecules to use for crosslinking, maleimide chemistry

3.2 FOP Project

3.2.1 Cloning and Expression Experiments of FOP Related Constructs

In conjunction with Dr. Nicholas W. Callahan, the tags present on the five FOP related constructs were modified on their N-terminal end. Beginning with the construction of a His-tagged variant, each construct was ligated into a pHLIC vector that did not contain a PelB leader sequence.

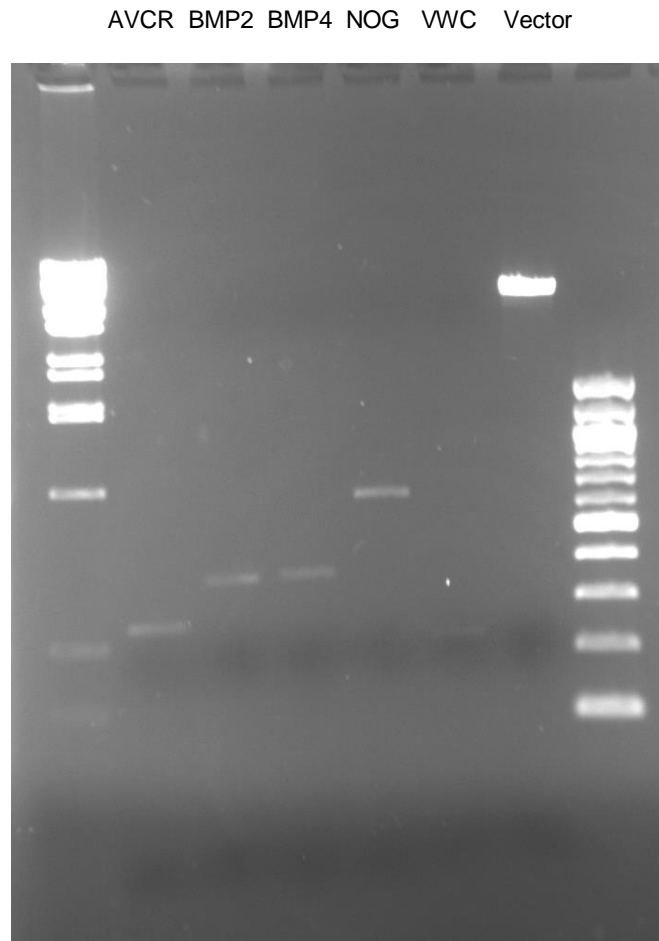


Figure 23 Gene construct containing inserts ready for ligation Into pHLIC vector.

These His-tagged variants were tested for expression in BL21 (DE3) cells. In this experiment, cells transformed with BMP4 did not grow and BMP4 was not expressed.

However, as it was predetermined by a different expression experiment, these proteins all express in the pellet. So these constructs underwent lysis in unfolding buffer and then purified on a Ni-NTA column, the protein was washed and eluted off in the presence of 8 M urea at pH 6 and pH 4, respectively. As shown in Figure 24, BMP2 and NOG both effectively expressed in BL21 cells and were purified. VWC and ACVR did not express in BL21 cells but were expressed by Dr. Nicholas W. Callahan in C43 (DE3) cells later.

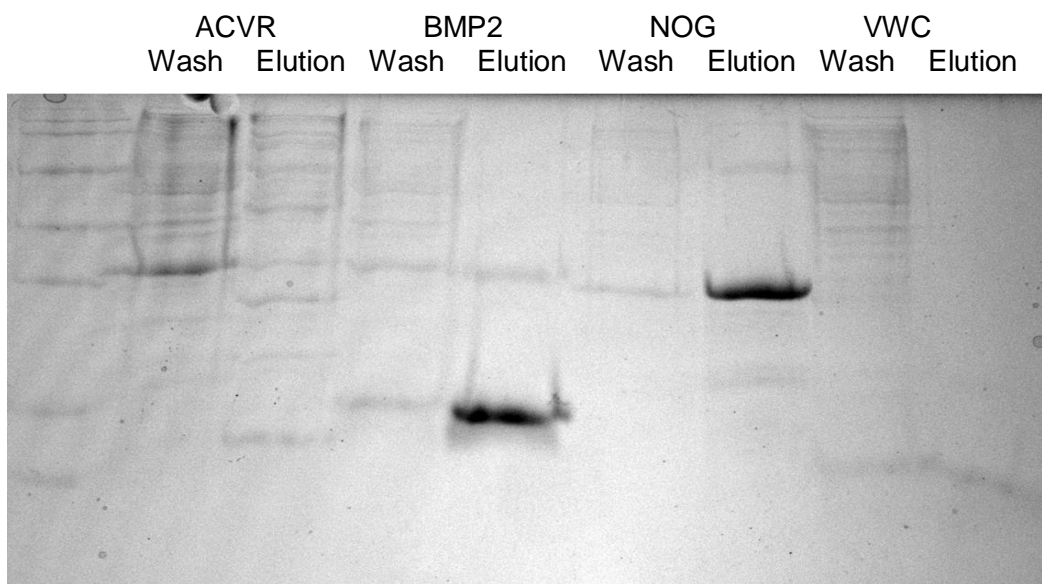


Figure 24 Expression of FOP related constructs in BL21 (DE3) cells

3.2.2 *PelB-His-tagged vs His-tagged vs Untagged*

When the untagged variants of each FOP related protein were created by removing the His tag sequence from each variant via PCR by Dr. Nicholas W. Callahan, all the constructs and their variants were tested for which exhibited the best expression. With BMP2, BMP4, and NOG transformed into BL21 cells and ACVR and VWC transformed into C41 (DE3) cells, a time controlled small scale expression experiment was performed.

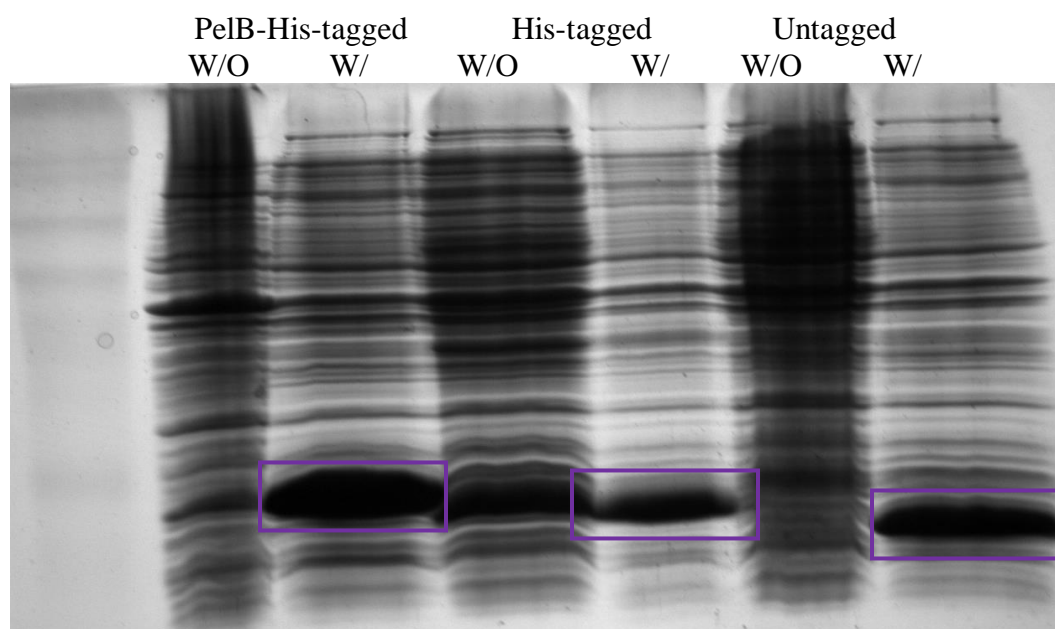


Figure 25 BMP2 expressed in BL21 cells without and with 100 μ M IPTG

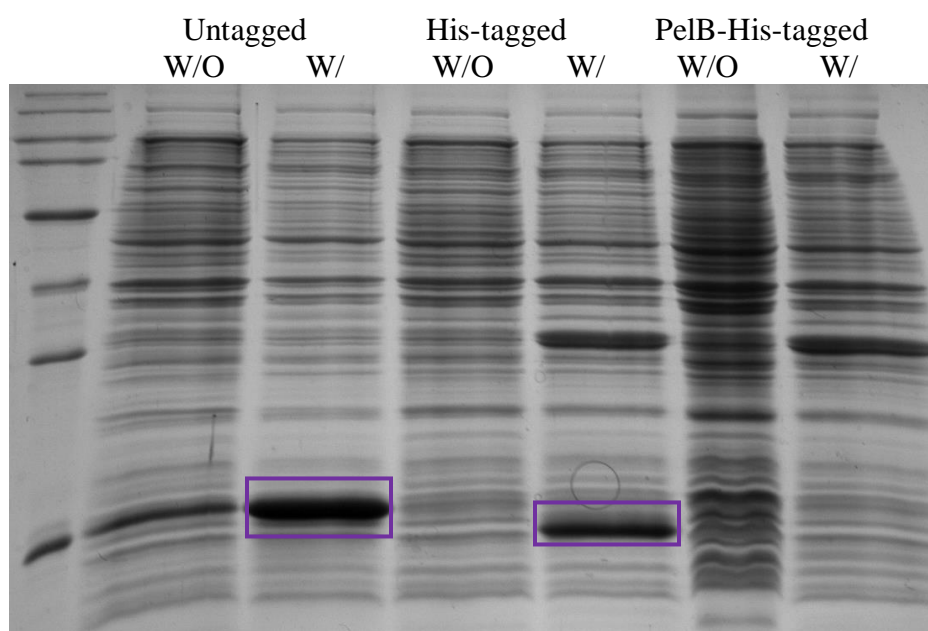


Figure 26 BMP4 expressed in BL21 cells without and with 100 μ M IPTG

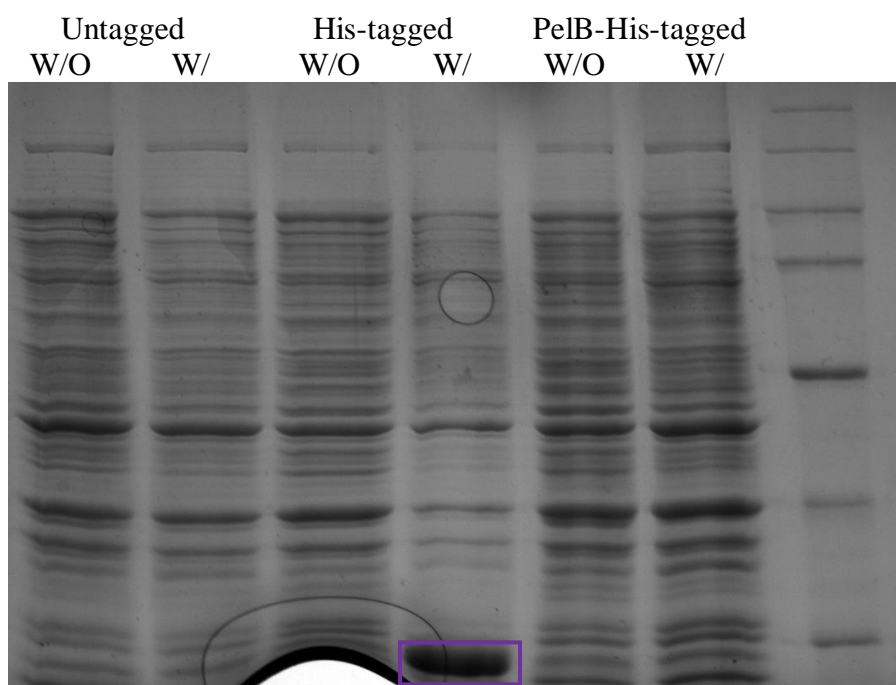


Figure 27 NOG expressed in BL21 cells without and with 100 μ M IPTG

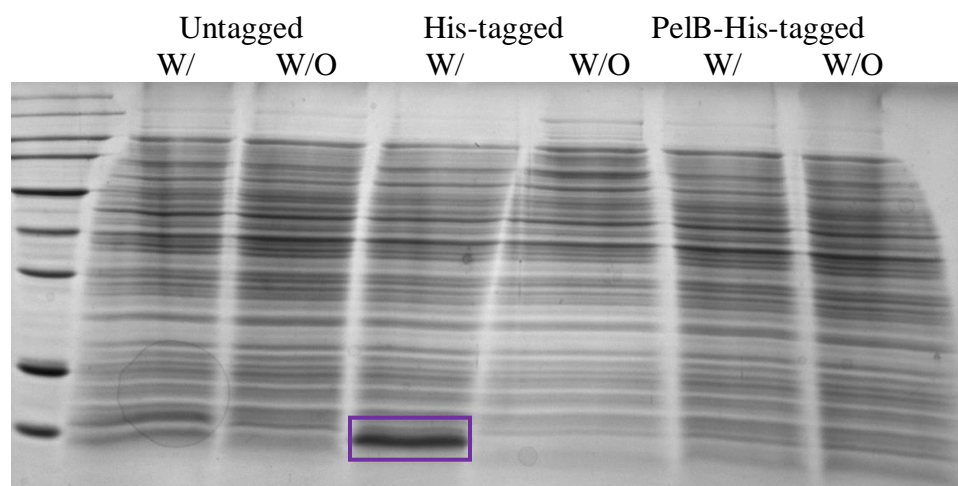


Figure 28 VWC expressed in C41 cells with and without 100 μ M IPTG

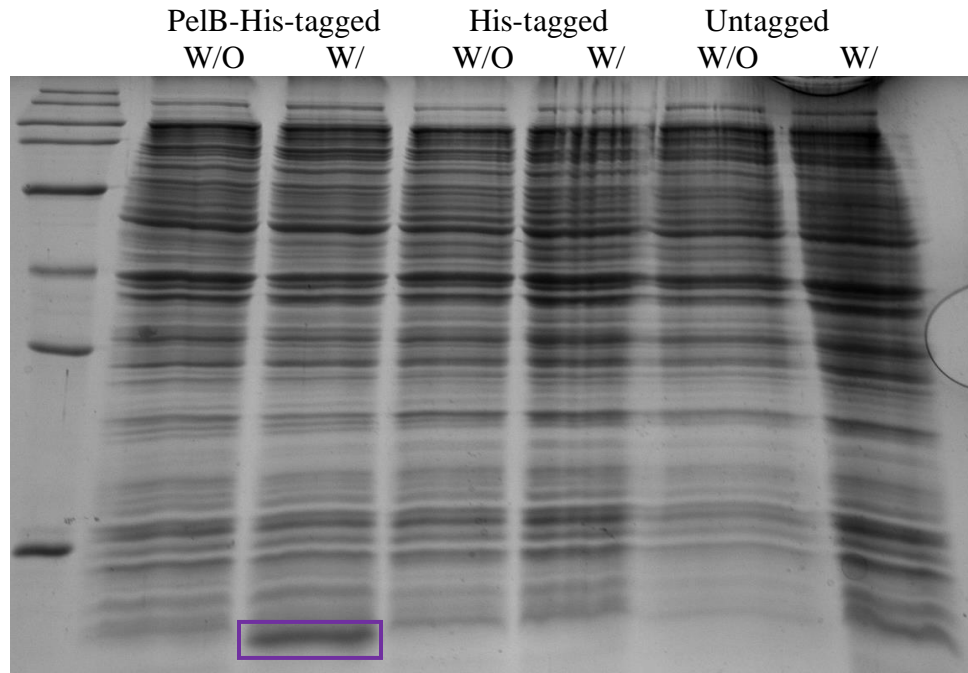


Figure 29 ACVR expressed in C41 (DE3) cells without and with 100 μ M IPTG

In the BL21 (DE3) cell line, all three variants of BMP2 expressed well, only the untagged and the His-tagged variants of BMP4 expressed, and only the His-tagged NOG variant expressed. For best purification methods, the His-tagged variants for these three constructs could be expressed well in BL21 (DE3) cells. BMP4 in later experiments expressed better while it is tagged. From the C41 (DE3) cell line, VWC only expressed with a His-tag while ACVR only expressed with the PelB-His-tag. Expressions of these constructs, like those with the notch project, seem to express best by aggregating in the cells. Due to this hindrance, re-folding techniques such as those used in the Notch project, must be used to retrieve a soluble, folded protein to work with for binding studies and crystallography.

Conclusions and Future Directions

With these additional constructs for both the Notch and FOP projects, a better understanding of which constructs can be efficiently expressed in *E. coli* and purified was determined. For the Notch project, the truncated and altered DLL1 constructs will be tested for binding affinity to the Notch 1 receptor through SPR. Additionally, these constructs will be used in in vitro assays done by the collaboration with the Dikov laboratory. For the FOP project, the human constructs that were determined to express the best in *E. coli* will continue to be used as the best method for expression for future binding and characterization studies. The Magliery laboratory hopes to continue research in both of these projects to acquire more insight into the proteins associated with both the Notch signaling pathway in cancer and Fibrodysplasia Ossificans Progressiva, respectively.

References

1. Lavinder, J.J.; Hari, S.B.; Sullivan, B.J.; Magliery, T.J. (2009) "High-Throughput Thermal Scanning: a general, rapid dye-binding thermal shift screen for protein engineering," *J. Am. Chem. Soc.* **131**: 3794-3795.
2. Allenspach, E. J., and Maillard, I. (2002). Notch Signaling in Cancer. *Cancer Biology & Therapy*, 1(5), 460. doi: 10.4161/cbt.1.5.159
3. Artavanis-Tsakonas, S., Rand, M.D., and Lake, R.J. (1999). Notch signaling: cell fate control and signal integration in development. *Science* 284, 770-776.
4. Binnerts, M. E., Wen, X., Canté-Barrett, K., Bright, J., Chen, H. T., Asundi, V., ... & Rupp, F. (2004). Human Crossveinless-2 is a novel inhibitor of bone morphogenetic proteins. *Biochemical and biophysical research communications*, 315(2), 272-280.
5. Chaikuad, A., Alfano, I., Kerr, G., Sanvitale, C. E., Boergemann, J. H., Triffitt, J. T., ... & Bullock, A. N. (2012). Structure of the bone morphogenetic protein receptor ALK2 and implications for fibrodysplasia ossificans progressiva. *Journal of Biological Chemistry*, 287(44), 36990-36998.
6. Chantler, P. D., & Bower, S. M. (1988). Cross-linking between translationally equivalent sites on the two heads of myosin. Relationship to energy transfer results between the same pair of sites. *Journal of Biological Chemistry*, 263(2), 938-944.
7. Chillakuri, C. R., Sheppard, D., Lea, S. M., and Handford, P. A. (2012). Notch receptor–ligand binding and activation: Insights from molecular studies. *Seminars in Cell & Developmental Biology*, 23(4), 421–428. doi:10.1016/j.semcdb.2012.01.009
8. Choi, J. H., & Lee, S. Y. (2004). Secretory and extracellular production of recombinant proteins using *Escherichia coli*. *Applied microbiology and biotechnology*, 64(5), 625-635.
9. Fortini, M. E. (2009). Notch Signaling: The Core Pathway and Its Posttranslational Regulation. *Developmental Cell*, 16(5), 633-47. doi: 10.1016/j.devcel.2009.03.010 Gridley, T. (2003). Notch signaling and inherited disease syndromes. *Hum. Mol. Genet.* 12, R9-R13.

10. Glaser, D. L., Economides, A. N., Wang, L., Liu, X., Kimble, R. D., Fandl, J. P., Wilson, J. M., Stahl, N., Kaplan, F. S., and Shore, E. M. (2003). In vivo somatic cell gene transfer of an engineered noggin mutein prevents BMP4-induced heterotopic ossification. *The Journal of Bone and Joint Surgery*, 85(12), 2332-2342.
11. Hermanson, G. T. (2013). *Bioconjugate techniques*. Academic press.
12. Huang, Y., Lin, L., Shanker, A., Malhotra, A., Yang, L., Dikov, M.M., and Carbone, D.P. (2011). Resuscitating cancer immunosurveillance: Selective stimulation of DLL1-Notch signaling in T cells rescues T-cell function and inhibits tumor growth. *American Association for Cancer Research*, 71(19), 6122-6129.
13. Kageyama, R., Ohtsuka, T., Shimojo, H., & Imayoshi, I. (2008). Dynamic Notch signaling in neural progenitor cells and a revised view of lateral inhibition. *Nature neuroscience*, 11(11), 1247-1251.
14. Luca, V. C., Jude, K. M., Pierce, N. W., Nachury, M. V., Fischer, S., & Garcia, K. C. (2015). Structural basis for Notch1 engagement of Delta-like 4. *Science*, 347(6224), 847-853.
15. Mayhew, M., Handford, P., Baron, M., Tse, A., Campbell, I., and Brownlee, G., (1992). Ligand requirements for Ca²⁺ binding to EGF-like domains. *Protein Engineering*, 5(6), 489-494.
16. Mohr, O.L. (1919). Character changes caused by mutation of an entire region of a chromosome in *Drosophila*. *Genetics* 4, 275-282.
17. Morgan, T.H., and Bridges, C.B. (1916). Sex-linked inheritance in *Drosophila*. *Pubis Carnegie Instn* 237, 1-88.
18. Nakayama, K., Nagase, H., Koh, C. S., & Ohkawara, T., (2013). γ -Secretase: Regulated signaling and Alzheimer's disease. In I. Serr (Ed.), *Understanding Alzheimer's Disease*. ISBN: 978-953-51-1009-5, InTech, DOI: 10.5772/54230. Available from: <http://www.intechopen.com/books/understanding-alzheimer-s-disease/-secretase-regulated-signaling-and-alzheimer-s-disease>
19. Nickel, J., Sebald, W., Groppe, J. C., & Mueller, T. D. (2009). Intricacies of BMP receptor assembly. *Cytokine & growth factor reviews*, 20(5), 367-377.
20. Pignolo, R. J., Shore, E. M., & Kaplan, F. S. (2013). Fibrodysplasia ossificans progressiva: diagnosis, management, and therapeutic horizons. *Pediatric endocrinology reviews: PER*, 10(0 2), 437.

21. Schumacher, F. F., Nobles, M., Ryan, C. P., Smith, M. E., Tinker, A., Caddick, S., & Baker, J. R. (2011). In situ maleimide bridging of disulfides and a new approach to protein PEGylation. *Bioconjugate chemistry*, 22(2), 132-136.
22. Shanker, A. (2013). Tuning NOTCH. *J Blood Lymph*, 3, e112.
23. Shanker, A., Dudimah, D. F., Pellom Jr, S. T., Uzhachenko, R. V., Carbone, D. P., & Dikov, M. M. (2014). Cancer therapy by resuscitating Notch immune surveillance. *Journal for immunotherapy of cancer*, 2(Suppl 1), P88.
24. Taylor, K. R., Vinci, M., Bullock, A. N., & Jones, C. (2014). ACVR1 mutations in DIPG: lessons learned from FOP. *Cancer research*, 74(17), 4565-4570.
25. Vu, T. T. T., Jeong, B., Yu, J., Koo, B. K., Jo, S. H., Robinson, R. C., & Choe, H. (2014). Soluble prokaryotic expression and purification of crotonamine using an N-terminal maltose-binding protein tag. *Toxicon*, 92, 157-165.
26. Zhang, J. L., Qiu, L. Y., Kotzsch, A., Weidauer, S., Patterson, L., Hammerschmidt, M., ... & Mueller, T. D. (2008). Crystal structure analysis reveals how the Chordin family member crossveinless 2 blocks BMP-2 receptor binding. *Developmental cell*, 14(5), 739-750.
27. Zimmer, J., Doelken, S. C., Horn, D., Groppe, J. C., Shore, E. M., Kaplan, F. S., & Seemann, P. (2012). Functional analysis of alleged NOGGIN mutation G92E disproves its pathogenic relevance. *PloS one*, 7(4), e35062.
28. Zhou, Y., Nie, W., Zhao, J., & Yuan, X. (2013). Rapidly in situ forming adhesive hydrogel based on a PEG-maleimide modified polypeptide through Michael addition. *Journal of Materials Science: Materials in Medicine*, 24(10), 2277-2286.